J. Fluid Mech. (1986), *vol.* 168, *pp.* 1–30
Printed in Great Britain

Absorption of sound at a slot in a splitter plate in a mean-flow duct

By M. C. QUINN
University of Southampton SO9 5NH, UK

AND M. S. HOWE
B.B.N. Laboratories, 10 Moulton Street, Cambridge, MA 02238, USA

(Received 29 June 1985)

Perforated screens are often deployed to attenuate aerodynamic sound in heat-exchanger cavities and other ducts conveying mean flow. The dissipation is caused by vorticity production in the perforations. This mechanism is investigated theoretically for the case of a thin rigid plate lying along the centreline of a duct and having a single transverse slot, a configuration that is to be studied experimentally at the Institute of Sound and Vibration Research of Southampton University. Time-harmonic acoustic waves are incident on the slot in the presence of equal parallel mean flows on either side of the plate. A linearized theory of unsteady shearing flow over a slot, which incorporates the influence of vorticity ejection into the flow, is used to examine mean-flow/acoustic energy exchanges. According to this theory acoustic energy is absorbed provided that the Strouhal number based on slot width and mean-flow velocity is sufficiently small. At higher frequencies there exists an infinite set of discrete frequency intervals within which there is a net production of acoustic energy at the slot at the expense of the kinetic energy of the mean flow.

1. Introduction

Perforated screens are used to suppress flow-induced acoustic resonances in ducts, heat-exchanger cavities and other industrial devices conveying mean flow (Bechert 1979; Blevins 1984; Vér 1982). A detailed analysis of several idealized model problems (Howe 1980*a*, *b*; 1981*a*, *b*) reveals that their effectiveness is due to vorticity production within the perforations by the sound, the kinetic energy of the vortex field being extracted from the sound. The vorticity is ejected from the perforations and convected downstream by the mean flow where it is subsequently dissipated by viscous action, although it sometimes happens that, after ejection, the efficiency of the acoustic dissipation is diminished because of the generation of sound ('aerodynamic sound', see Lighthill 1952) by the vorticity interacting with other perforations.

An experimental investigation is underway in the Institute of Sound and Vibration Research of Southampton University to examine such mean-flow/acoustic interactions (Vasudevan, Nelson & Howe 1985). A canonical configuration will first be examined in which the perforated screen consists of a single transverse slot in a thin rigid plate lying along the centreline of a duct of rectangular cross-section. On each side of the plate are equal, parallel, low-subsonic mean flows. Two time-harmonic acoustic waves of equal amplitudes but of phase difference θ are generated by a system of loudspeakers, and are incident on the slot from upstream, respectively above and below the splitter plate. In this paper we apply the linearized theory of unsteady

shearing flow over a slot, discussed by Howe (1981*b*), to an idealized model of this experimental configuration. The shear layer within the slot is treated as a vortex sheet and the back-reaction on the flow in the slot of vorticity ejected from the slot trailing edge is expressed in terms of displacement-thickness 'waves' on the downstream boundary layers. These displacement waves constitute an attempt to model the influence of the ejected vorticity that is being convected by the mean flow, and it turns out that, on the basis of linear theory, their amplitudes can be determined analytically by imposing the condition that the displacement of the shear layer within the slot should remain finite at the trailing edge.

Attention will be confined to configurations, relevant in the experimental study, in which the slot width does not exceed the width of the duct, and to the compact case in which both are small compared with the characteristic acoustic wavelength. The analytical problem is formulated in §2. A solution is first obtained in §3 which takes no account of vorticity ejection from the slot. The general case of arbitrary $s/H < 1$, where $2s$, $2H$ are respectively the widths of slot and duct, is treated in §3.1 and the problem is reduced to the consideration of a set of linear equations which are solved numerically. The solution is given in closed form in §3.2 for $s^2/H^2 \ll 1$. The displacement ζ, say, of the vortex sheet from its undisturbed position contains two terms which represent degenerate Kelvin–Helmholtz instability waves. Since there is no mean shear one of these waves is neutrally stable while the second grows linearly with distance downstream. Their amplitudes are determined by application of the unsteady Kutta condition at the leading edge of the slot, leaving conditions at the trailing edge to be determined by the solution. The predicted motion of the shear layer at the trailing edge exhibits an inverse square-root singularity. Accordingly the linearized solution breaks down in the vicinity of the trailing edge.

The singularity is removed in §4 by the incorporation of displacement-thickness waves, whose amplitude is adjusted to ensure that the motion remains finite at the trailing edge. This, moreover, leads to a solution in which ζ is not only finite but merges continuously at the trailing edge with the boundary-layer-displacement waves.

The acoustic properties of the slot are determined by the unsteady flux through it, and this is shown to have two components: the first is distributed and is caused by the to-and-fro motion of the vortex sheet; the second is localized at the trailing edge of the slot and is associated with the ejection of vorticity. The mean-flow/acoustic energy exchanges are examined in §§5 and 6. It is concluded that, for Strouhal numbers $\omega s/U$ less than about 2.4 (where ω is the radian frequency and U the velocity of the mainstream), acoustic energy is dissipated and, provided that $\omega s/U$ is not too small, the dissipation decreases as s/H increases. Predictions are given of Δ, the ratio of transmitted to *net* incident power flux, (to be determined in the experiment) for various phase differences and s/H ratios. Measurable values of Δ are found for phase differences θ in the range $\frac{3}{4}\pi \leqslant \theta \leqslant \pi$, the maximum being achieved at $\theta = \pi$ where $\Delta = O(10)$ dB for $\omega s/U \ll 1$. The derivations of various analytical results are collected together in Appendices A–D.

2. Formulation of the analytical problem

Consider a two-dimensional rigid-walled duct of width $2H$ which occupies the region $-\infty < x_1 < \infty$, $|x_2| \leqslant H$ of a rectangular co-ordinate system (x_1, x_2) (see figure 1). A thin rigid plate lies along the centreline $x_2 = 0$ of the duct and has a single transverse slot of length $2s$, centred on the origin of coordinates. In the undisturbed

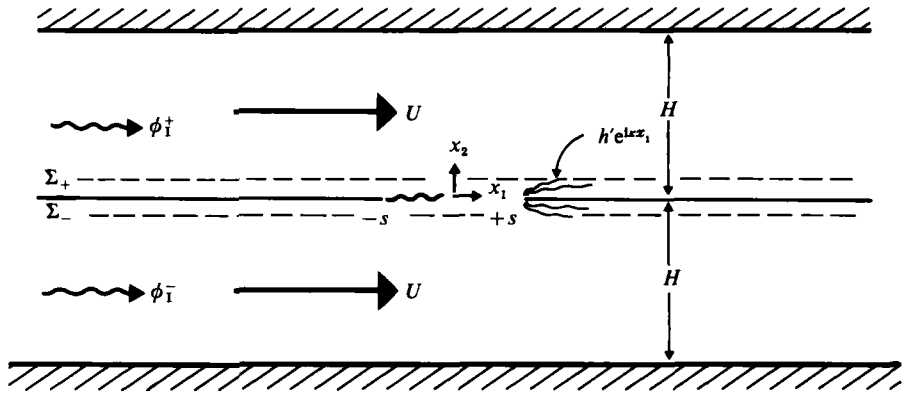

FIGURE 1. Schematic illustration of the analytical problem.

state the fluid on either side of this plate is in uniform motion at low-subsonic velocity U in the positive x_1-direction.

Plane time-harmonic sound waves of radian frequency $\omega > 0$ are incident on the slot from upstream and are specified by the velocity potentials

$$\left.\begin{aligned} \phi_I^+ &= \phi_0 \exp\left\{\mathrm{i}\left[\frac{kx_1}{1+M} - \omega t\right]\right\} \quad (x_2 > 0), \\ \phi_I^- &= \phi_0 \exp\left\{\mathrm{i}\left[\frac{kx_1}{1+\mathrm{M}} - \omega t - \theta\right]\right\} \quad (x_2 < 0), \end{aligned}\right\} \tag{2.1}$$

where ϕ_0 is a constant, $k = \omega/c$ is the acoustic wavenumber, θ is the phase difference of the incident waves (which can be varied by suitable adjustment of the loudspeaker system), $M = U/c \ll 1$ is the Mach number of the mean flow and c is the speed of sound. It is assumed that c and the mean density ρ_0 of the fluid are constant throughout the flow, and that

$$M \ll 1, \quad ks \leqslant kH \ll 1. \tag{2.2}$$

This implies that the characteristic wavelength of the sound greatly exceeds the respective widths $2s$, $2H$ of the slot and duct, and that the frequency is below the minimum cut-on frequencies of transverse duct modes.

To analyse the flow–acoustic interactions at the slot we introduce Green functions $G_\pm(\boldsymbol{x}, y_1)$ which, in view of (2.2), satisfy the time-reduced wave equation:

$$\left[\frac{\partial^2}{\partial x_1^2} + \frac{\partial^2}{\partial x_2^2} + \left(k - \mathrm{i}M\frac{\partial}{\partial x_1}\right)^2\right] G_\pm(\boldsymbol{x}, y_1) = 0 \quad (x_2 \gtrless 0),$$

the boundary conditions

$$\left.\begin{aligned} \frac{\partial G_\pm}{\partial x_2} &= \pm\delta(x_1 - y_1) \quad (-\infty < x_1 < \infty, x_2 = \pm 0), \\ \frac{\partial G_\pm}{\partial x_2} &= 0 \quad (-\infty < x_1 < \infty, x_2 = \pm H), \end{aligned}\right\} \tag{2.3}$$

and the radiation condition that $G_\pm$ exhibit outgoing wave behaviour as $|x_1 - y_1| \to \infty$. Explicit forms for $G_\pm$ are derived in Appendix A.

Let $\Sigma_\pm$ denote plane control surfaces $x_2 = \pm\delta$ which lie just outside regions of

unsteady vortical flow above and below the splitter plate. If $Z_\pm(x_1)\,\mathrm{e}^{-\mathrm{i}\omega t}$ respectively denote the displacement of fluid particles in $\Sigma_\pm$ from their unperturbed positions, the corresponding perturbation potentials $\phi_\pm$ induced by the motion of the shear layer and displacement-thickness fluctuations of the boundary layers on the splitter plate can be expressed in the form

$$\phi_\pm(\boldsymbol{x}) = \pm\left(-\mathrm{i}\omega + U\frac{\partial}{\partial x_1}\right)\int_{-\infty}^{\infty} Z_\pm(y_1)\,G_\pm(\boldsymbol{x}, y_1)\,\mathrm{d}y_1. \tag{2.4}$$

Here and henceforth the exponential time factor $\mathrm{e}^{-\mathrm{i}\omega t}$ is suppressed and it is assumed that the lengthscale of variation of $Z_\pm(y_1)$ greatly exceeds the thickness of the boundary-layer flows, so that the integrations in (2.4) may be taken along $x_2 = \pm 0$ respectively. The linearized Bernoulli equation may now be used to show that the total perturbation pressures $p_\pm$ in $x_2 \gtrless 0$ are given by

$$p_\pm(\boldsymbol{x}) = \mp\rho_0\left(-\mathrm{i}\omega + U\frac{\partial}{\partial x_1}\right)^2\int_{-\infty}^{\infty} Z_\pm(y_1)\,G_\pm(\boldsymbol{x}, y_1)\,\mathrm{d}y_1 + p_0^\pm, \tag{2.5}$$

where, since $M \ll 1$,

$$p_0^+ = -\mathrm{i}\rho_0\omega\phi_0\,\mathrm{e}^{\mathrm{i}kx_1/(1+M)}, \tag{2.6}$$

$$p_0^- = -\mathrm{i}\rho_0\omega\phi_0\,\mathrm{e}^{\mathrm{i}(kx_1/(1+M)-\theta)}, \tag{2.7}$$

are the pressures due to the incident waves $\phi_{\mathrm{I}}^\pm$.

The shear layer within the slot will be modelled by a vortex sheet, so that for $|x_1| < s$ we can set

$$Z_+(x_1) = Z_-(x_1) = Z(x_1), \tag{2.8}$$

say. In a linearized approximation the pressure $p(\boldsymbol{x})$ may be taken to be continuous across the mean position of the vortex sheet, i.e.

$$p_+(x_1, +0) = p_-(x_1, -0) \quad (|x_1| < s), \tag{2.9}$$

whence it follows from (2.5) that

$$\frac{p_0}{\rho_0} = \left\{-\mathrm{i}\omega + U\frac{\partial}{\partial x_1}\right\}^2\int_{-\infty}^{\infty}\{Z_+(y_1)\,G_+(\boldsymbol{x}, y_1)|_{x_2=0+} + Z_-(y_1)\,G_-(\boldsymbol{x}, y_1)|_{x_2=0-}\}\,\mathrm{d}y_1 \quad (|x_1| < s), \tag{2.10}$$

where, from (2.6) and (2.7),

$$p_0 = p_0^+ - p_0^- = -\mathrm{i}\rho_0\omega\phi_0\,\mathrm{e}^{\mathrm{i}kx_1/(1+M)}\{1-\mathrm{e}^{-\mathrm{i}\theta}\}.$$
$$\approx -\mathrm{i}\rho_0\omega\phi_0(1-\mathrm{e}^{-\mathrm{i}\theta}), \tag{2.11}$$

since $k|x_1| \leqslant ks \ll 1$.

For $x_1 > s$, $Z_\pm$ is the x_2 displacement of fluid particles just outside the boundary layers. We shall assume, following Howe (1981*b*), that long-wavelength boundary-layer disturbances are adequately represented by

$$Z_\pm = h'_\pm\,\mathrm{e}^{\mathrm{i}\kappa x_1} \quad \left(\kappa = \frac{\omega}{V}, \quad x_1 > s\right), \tag{2.12}$$

where $h'_\pm$ are constants, and $V \leqslant U$ is a suitable convection velocity of the boundary-layer disturbances. Further discussion and justification for this approach

is given by Howe (1981*b*, *c*), who also shows that at low-subsonic flow velocity, conservation of mass requires that $h'_+ = h'_- = h'$, say. Since conditions upstream of the slot are homogeneous, and displacement-thickness waves propagate in the flow direction, it may be assumed that $Z_\pm = 0$ for $x_1 < -s$.

It is convenient to introduce dimensionless variables, as follows:

$$\left.\begin{aligned} \xi &= \frac{x_1}{s}, \quad \eta = y_1/s, \\ \zeta &= \frac{Z}{s}, \quad \zeta_\pm = h\,\mathrm{e}^{\mathrm{i}\sigma\xi}, \quad \sigma = \kappa s \end{aligned}\right\} \tag{2.13}$$

and dimensionless fluxes

$$Q = q_0 + q_h \tag{2.14}$$

defined by

$$q_0 = \int_{-1}^{+1} \zeta(\xi)\,\mathrm{d}\xi \quad q_h = h\int_{+1}^{\infty} \mathrm{e}^{\mathrm{i}\sigma\xi}\,\mathrm{d}\xi = -\frac{h\,\mathrm{e}^{\mathrm{i}\sigma}}{\mathrm{i}\sigma}. \tag{2.15a, b}$$

Q is the total displacement flux through the slot, and consists of a component q_0 arising from the motion of the vortex sheet, together with q_h, which accounts for a flux through an infinitesimal length of the slot adjacent to the trailing edge and is associated with the production of the displacement-thickness waves (see Howe 1981*b*). Note that the convergence of infinite integrals of the type shown in (2.15*b*) may be achieved by assigning to ω a small positive imaginary component (subsequently allowed to vanish). This procedure is consistent with the causality condition that displacement-thickness fluctuations are *produced* by the incident sound and would in practice decay (or become incoherent) as they propagate downstream.

When the inequalities (2.2) are satisfied the Green functions G_+, G_- assume a common form in the acoustic near field of the slot, namely

$$\left.\begin{aligned} G_\pm(\boldsymbol{x}, y)|_{x_2 = 0_\pm} &= \frac{1}{\pi}\ln\left\{\sinh\left\{|x_1 - y_1|\frac{\pi}{2H}\right\}\right\} + c_\pm \\ \text{where} \qquad c_\pm &= -\frac{\mathrm{i}}{2Hk} + \frac{\ln 2}{\pi} \end{aligned}\right\} \tag{2.16}$$

(see Appendix A).

Substituting into (2.10) and rewriting in terms of dimensionless variables we deduce that the displacement ζ of the vortex sheet is given by the integro–differential equation

$$\left(-\mathrm{i}\epsilon + \frac{\partial}{\partial\xi}\right)^2\left[(c_+ + c_-)Q + \frac{2}{\pi}\int_{-1}^{+1}\zeta(\eta)\ln\left\{\sinh\left(|\xi-\eta|\frac{\pi s}{2H}\right)\right\}\mathrm{d}\eta\right.$$
$$\left. + \frac{2}{\pi}\int_{+1}^{\infty} h\,\mathrm{e}^{\mathrm{i}\sigma\eta}\ln\left\{\sinh\left(|\xi-\eta|\frac{\pi s}{2H}\right)\right\}\mathrm{d}\eta\right] = \frac{p_0}{\rho_0 U^2} \quad (|\xi| < 1), \tag{2.17}$$

where $\epsilon = \omega s/U$ is the Strouhal number based on slot width and mean-flow velocity. This equation determines $\zeta(\xi, t)$ correct to neglect of terms $O(ks)$, $O(ksM)$ relative to unity, which represents the orders of magnitude of terms neglected in using the

approximations (2.11) for p_0 and (2.16) for $G_{\pm}(x, y)$. Integration with respect to the differential operator yields

$$\int_{-1}^{+1} \zeta(\eta) \ln\left\{\sinh\left(|\xi-\eta|\frac{\pi s}{2H}\right)\right\} \mathrm{d}\eta = -\frac{\pi p_0}{2\rho_0 U^2\epsilon^2} - \tfrac{1}{2}\pi Q\,(c_+ + c_-) + (\alpha\xi+\beta)\,\mathrm{e}^{\mathrm{i}\epsilon\xi}$$
$$-\int_{+1}^{\infty} h\,\mathrm{e}^{\mathrm{i}\sigma\eta} \ln\left\{\sinh\left(|\xi-\eta|\frac{\pi s}{2H}\right)\right\} \mathrm{d}\eta \quad (|\xi|<1). \tag{2.18}$$

In this result α, β are constants denoting the amplitudes of the degenerate Kelvin–Helmholtz instability waves on the vortex sheet. The values of α, β and the displacement-thickness wave amplitude h are to be chosen to ensure that the Kutta condition is satisfied at the leading edge, $\xi = -1+0$, of the slot, i.e. at the *trailing edge* of the upstream portion of the splitter plate (as in classical thin-airfoil theory), and that ζ is finite at the slot trailing edge.

We shall obtain the solution of (2.18) only for $s \leqslant H$, which represents the most important case in practice. To do this it is convenient to employ the following expansion of the kernel of the integral equation:

$$\ln\left\{\sinh\left(|x|\frac{\pi s}{2H}\right)\right\} = \ln\frac{\pi s}{2H} + \ln|x| + P(x) \quad \left(\frac{|x|s}{2H}<1\right), \tag{2.19}$$

where

$$P(x) = \sum_{n=1}^{\infty} c_{2n}\,x^{2n}, \tag{2.20}$$

$$c_{2n} = \frac{(-1)^{n-1}B_n}{(2n)\,(2n)!}\left(\frac{\pi s}{2H}\right)^{2n} 2^{2n} \tag{2.21}$$

and the B_n, $n \geqslant 1$, are the Bernoulli numbers ($\frac{1}{6}, \frac{1}{30}, \frac{1}{42}, \frac{1}{30}, \frac{5}{66}, \ldots$) (see, e.g., Abramowitz & Stegun 1964 §4.5).

3. Case I: no displacement-thickness waves

When no account is taken of periodic vorticity ejection from the trailing edge of the slot into the boundary layers in $x_1 > s$, we take $h = 0$ in (2.18). In this case it is possible to satisfy the Kutta condition at the leading edge of the slot, but ζ will turn out to be unbounded at the downstream end. When $h \equiv 0$ the expansion (2.19) permits the integral equation (2.18) to be expressed in the form

$$\int_{-1}^{+1} \zeta(\eta) \ln|\xi-\eta|\,\mathrm{d}\eta = \chi_0(\xi) + \chi_1(\xi) = \chi(\xi), \tag{3.1}$$

where

$$\chi_0(\xi) = -\frac{\pi p_0}{2\rho_0 U^2\epsilon^2} - q_0\left\{\frac{\pi}{2}(c_+ + c_-) + \ln\frac{\pi s}{2H}\right\} + (\alpha\xi+\beta)\,\mathrm{e}^{\mathrm{i}\epsilon\xi}, \tag{3.2}$$

$$\chi_1(\xi) = -\int_{-1}^{+1} \zeta(\eta)\,P(\xi-\eta)\,\mathrm{d}\eta. \tag{3.3}$$

Equation (3.1) determines the displacement $\zeta(\xi)$ in terms of the pressure difference p_0 of the incident waves, the two unknown wave amplitudes α and β, and an infinite series of moments $q_0, q_1, \ldots, q_\infty$ of the flux given by

$$q_n = \int_{-1}^{+1} \xi^n \zeta(\xi)\,\mathrm{d}\xi. \tag{3.4}$$

The solution of (3.1) is formally given by

$$\zeta(\xi) = \frac{1}{\pi(1-\xi^2)^{\frac{1}{2}}\ln 2}\{\ln 2\,\Theta_1(\chi,\xi) - \Theta_0(\chi)\}, \tag{3.5}$$

where $\Theta_0(\chi)$ and $\Theta_1(\chi,\xi)$ are the linear functionals

$$\Theta_0(\chi) = \frac{1}{\pi}\int_{-1}^{+1}\frac{\chi(\eta)\,\mathrm{d}\eta}{(1-\eta^2)^{\frac{1}{2}}}, \quad \Theta_1(\chi,\xi) = \frac{1}{\pi}\int_{-1}^{+1}\frac{(1-\eta^2)^{\frac{1}{2}}\chi'(\eta)\,\mathrm{d}\eta}{(\eta-\xi)}, \tag{3.6}$$

the prime denoting differentiation with respect to η, and where the second integral is a principal value (Carrier, Krook & Pearson 1966, p. 428). The Kutta condition requires that the vortex sheet leaves the leading edge of the slot tangentially, i.e. that

$$\zeta(\xi), \quad \frac{\partial\zeta}{\partial\xi} \to 0 \quad \text{as} \quad \xi \to -1+0. \tag{3.7}$$

We anticipate from the work of Howe (1981*b*) that $\zeta = O(1+\xi)^{\frac{3}{2}}$ as $\xi \to -1+0$.

When (3.5) is integrated with respect to ξ over the slot the contribution from Θ_1 vanishes, and it follows that

$$q_0 + \frac{\Theta_0(\chi)}{\ln 2} = 0. \tag{3.8}$$

This result permits conditions (3.7) to be written in the form

$$\left.\begin{aligned} &\lim_{\xi\to-1+0}\{q_0+\Theta_1(\chi,\xi)\} = 0, \\ \text{and} \qquad &\lim_{\xi\to-1+0}\frac{\partial\Theta_1}{\partial\xi}(\chi,\xi) = 0, \end{aligned}\right\} \tag{3.9}$$

(see Howe 1981*b*, §2).

The linear functionals Θ_1, Θ_0 involve the unknown moments $q_0, q_1, q_2, \ldots$ which are determined by multiplying (3.5) by ξ^n ($n = 0, 1, 2, \ldots$) and integrating over the slot. This leads to an infinite system of linear algebraic equations which, when combined with boundary conditions (3.9), are sufficient to determine the unknown parameters $\alpha, \beta, q_0, q_1, \ldots$. In practice the infinite series defined by (2.20) is truncated after N terms, say, in which case $2N+3$ equations must be solved in terms of p_0 and the Strouhal number ϵ for the $(2N+3)$ unknowns $\alpha, \beta, q_0, \ldots, q_{2N}$. The procedure is described in §3.1 for arbitrary $s < H$. In §3.2 consideration is given to the particular case of $s \ll H$, which can be treated analytically. The following definitions will be employed:

$$\left.\begin{aligned} a_n &= \frac{1}{\pi}\int_{-1}^{+1}\frac{\xi^n\,\mathrm{d}\xi}{(1-\xi^2)^{\frac{1}{2}}}, \quad b_n(\xi) = \frac{1}{\pi}\int_{-1}^{+1}\frac{(1-\eta^2)^{\frac{1}{2}}\eta^n}{(\eta-\xi)}\,\mathrm{d}\eta, \\ d_n^m &= \frac{1}{\pi}\int_{-1}^{+1}\frac{\xi^m b_n(\xi)}{(1-\xi^2)^{\frac{1}{2}}}\,\mathrm{d}\xi, \quad f_m(\epsilon) = \frac{1}{\pi}\int_{-1}^{+1}\frac{\xi^m g(\epsilon,\xi)}{(1-\xi^2)^{\frac{1}{2}}}\,\mathrm{d}\xi, \end{aligned}\right\} \tag{3.10}$$

where $g(\epsilon,\xi) = \Theta_1(-\mathrm{e}^{\mathrm{i}\epsilon\eta},\xi)$ (see Appendix B), and the integral defining $b_n(\xi)$ is a principal value.

3.1. *Nth order calculation*

To perform the calculation correct to $O(\pi s/2H)^{2N}$ we must retain the first N terms of the infinite series P of (2.20). The functionals corresponding to χ_0, χ_1 are evaluated, respectively, in Appendices B and C. Substituting into (3.5) we obtain

$$\zeta(\xi) = \frac{1}{\pi \ln 2(1-\xi^2)^{\frac{1}{2}}}\left\{E + \left[\sum_{r=0}^{2N-1} q_r C(r,\xi)\right] + q_{2N} c_{2N} + \left[q_{-1} - \mathrm{i}q_{-2}\frac{\partial}{\partial\epsilon}\right]\mathscr{M}(\epsilon,\xi)\right\}, \tag{3.11}$$

in which we make the identification $\beta = q_{-1}$, $\alpha = q_{-2}$; ${}^nc_j$ denote the binomial coefficients and

$$\left.\begin{aligned} C(j,\xi) &= C_1(j) - \ln 2\, C_2(j,\xi), \\ C_1(j) &= (-1)^j \sum_{n=[j]}^{N} c_{2n}\, a_{2n-j}\, {}^{2n}c_j, \\ C_2(j,\xi) &= (-1)^j \sum_{n=[j+1]}^{n=N} 2n\, c_{2n}\, b_{2n-j-1}(\xi)\, {}^{2n-1}c_j, \end{aligned}\right\} \tag{3.12}$$

with

$$[j] = \begin{cases} 1 & (j \leqslant 2) \\ \frac{1}{2}j & (j \geqslant 4, j \text{ even}) \\ \frac{1}{2}(j+1) & (j \geqslant 3, j \text{ odd}) \text{ (see (C4)–(C5)).} \end{cases}$$

Also

$$\left.\begin{aligned} E &= \frac{p_0\pi}{2\rho_0 U^2\epsilon^2} + \tfrac{1}{2}q_0\pi(c_+ + c_-) + \ln\left(\frac{\pi s}{2H}\right), \\ \mathscr{M}(\epsilon,\xi) &= -(J_0(\epsilon) + \mathrm{i}\epsilon \ln 2\, g(\epsilon,\xi)), \end{aligned}\right\} \tag{3.13}$$

where $J_0(\epsilon)$ is the zeroth-order Bessel function.

$(2N+1)$ equations are now formed by multiplication of (3.11) by $\xi^m (m = 0, \ldots, 2N)$ and integration between $(-1, +1)$. It is convenient to adopt the normalization $\hat{q}_n = q_n/E$. Making use of the definitions (3.10) we obtain in this way

$$\begin{aligned} -a_m = &-\ln 2\, \hat{q}_m + \sum_{r=0}^{2N-1} \hat{q}_r\, B(m,r) + \hat{q}_{2N}\, c_{2N}\, a_m \\ &+ \left[\hat{q}_{-1} - \mathrm{i}\hat{q}_{-2}\frac{\partial}{\partial\epsilon}\right] A(m,\epsilon) \quad (m = 0, 1, \ldots, 2N), \end{aligned} \tag{3.14}$$

where for integer i, j

$$B(i,j) = (-1)^j\left[\sum_{n=[j]}^{N} c_{2n}\, a_{2n-j}\, {}^{2n}c_j\, a_i - \ln 2 \sum_{n=[j+1]}^{N} 2n\, c_{2n}\, d^i_{2n-j-1}\, {}^{2n-1}c_j\right], \tag{3.15a}$$

$$A(i,\epsilon) = -\{a_i J_0(\epsilon) + \mathrm{i}\epsilon \ln 2 f_i(\epsilon)\}. \tag{3.15b}$$

To simplify the two equations expressing the Kutta condition of (3.9) we introduce the summation term

$$D(j,\xi) = -\frac{\partial}{\partial\xi}C_2(j,\xi) = (-1)^j\left\{\sum_{n=[j+1]}^{N} 2n\, c_{2n}\frac{\partial}{\partial\xi} b_{2n-1-j}(\xi)\, {}^{2n-1}c_j\right\}, \tag{3.16}$$

after which (3.9), (3.11) yield

$$0 = \hat{q}_0 - \sum_{r=0}^{2N-1} \hat{q}_r C_2(r, -1) - \left[\hat{q}_{-1} - \mathrm{i}\hat{q}_{-2}\frac{\partial}{\partial\epsilon}\right] \mathrm{i}\epsilon g(\epsilon, -1), \tag{3.17}$$

$$0 = \sum_{r=0}^{2N-1} \hat{q}_r D(r, -1) + \left[\hat{q}_{-1} - \mathrm{i}\hat{q}_{-2}\frac{\partial}{\partial\epsilon}\right] \mathrm{i}\epsilon\frac{\partial}{\partial\xi} g(\epsilon, -1). \tag{3.18}$$

Equations (3.14), (3.17) and (3.18) are sufficient to determine $q_{-2}, q_{-1}, q_0, \ldots, q_{2N}$. In the numerical computation the value of N selected depends on s/H. For $s/H \ll 1$, $N = 1$ is enough, while for larger values of s/H an appropriate value of N is suggested by previous computations. N is then increased until the solution has converged (e.g. for $s/H = 0.7$ we take $N = 6$).

The zeroth-order moment q_0 determines the acoustic properties of the slot. Let $\hat{q}_0 = W(\epsilon)$, where the right-hand side is obtained by solution of the system (3.14), (3.17) and (3.18). From (3.13) it follows that

$$q_0 = \left\{\frac{\pi p_0}{2\rho_0 U^2\epsilon^2} + \tfrac{1}{2}q_0\pi(c_+ + c_-) + q_0 \ln\left(\frac{\pi s}{2H}\right)\right\} W(\epsilon). \tag{3.19}$$

Setting

$$F(\epsilon) = [W(\epsilon)]^{-1} - \ln\left(\frac{\pi s}{2H}\right) - \ln 2 \tag{3.20}$$

then leads to the following relation between the flux q_0 and the 'forcing' pressure p_0 of the incident waves;

$$q_0\{F(\epsilon) + \ln 2 - \tfrac{1}{2}\pi[c_+ + c_-]\} = \frac{\pi p_0}{2\rho_0 U^2\epsilon^2}. \tag{3.21}$$

It is not difficult to see that $F(\epsilon)$ is ultimately periodic with period π as $\epsilon \to \infty$. For instance, the influence of ϵ on the solution for $\hat{q}_0 = W(\epsilon)$ is limited to the 'coefficients' of the Helmholtz wave amplitudes q_{-1}, q_{-2} in (3.14), (3.17) and (3.18). As $\epsilon \to \infty$ all of those coefficients have the form $\epsilon^{\frac{1}{2}} \times f_{\mathrm{p}}$, where f_{p} is some function periodic in ϵ having period 2π, except for the term appearing in (3.18), namely $\mathrm{i}\epsilon(\partial/\partial\xi)\, g(\epsilon, -1) \sim \epsilon^{\frac{3}{2}} f_{\mathrm{p}}$ (see (B 3)). Kramer's rule then shows that $\hat{q}_0$ is ultimately periodic, and (3.19), (3.20) show that $F(\epsilon)$ must also become periodic, both with period π.

3.2. $s \ll H$ *first-order calculation*

If s/H is sufficiently small that terms $O((s/H)^m)$ $(m > 2)$ may be neglected, we can take $N = 1$ in the analysis of §3.1. Equations (3.14) become, for $m = 0, 1, 2$,

$$-1 = \hat{q}_0\{B(0, 0) - \ln 2\} + \hat{q}_1 B(0, 1) + \hat{q}_2 c_2 + \hat{q}_{-1} A(0, \epsilon) + \hat{q}_{-2}\left\{-\mathrm{i}\frac{\partial}{\partial\epsilon} A(0, \epsilon)\right\}, \tag{3.22}$$

$$0 = \hat{q}_0 B(1, 0) + \hat{q}_1[B(1, 1) - \ln 2] + \hat{q}_{-1} A(1, \epsilon) + \hat{q}_{-2}\left[-\mathrm{i}\frac{\partial}{\partial\epsilon} A(1, \epsilon)\right], \tag{3.23}$$

$$-\tfrac{1}{2} = \hat{q}_0 B(2, 0) + \hat{q}_1 B(2, 1) + \hat{q}_2\{\tfrac{1}{2}c_2 - \ln 2\} + \hat{q}_{-1} A(2, \epsilon) + \hat{q}_{-2}\left\{-\mathrm{i}\frac{\partial}{\partial\epsilon} A(2, \epsilon)\right\} \tag{3.24}$$

where, from (2.21), $c_2 = \frac{1}{6}(\pi s/2H)^2$.

The coefficients $B(i, j)$, $A(i, \epsilon)$ are calculated from (3.15a, b), making use of results (B 6), (C 1), (D 3):

$$B(0,0) = \tfrac{1}{2}c_2, \quad B(1,1) = -c_2 \ln 2, \quad B(1,0) = B(0,1) = B(2,1) = 0,$$
$$B(2,0) = \tfrac{1}{4}c_2(1+\ln 2), \quad A(0,\epsilon) = -J_0(\epsilon), \quad A(1,\epsilon) = -\mathrm{i}\ln 2 J_1(\epsilon),$$
$$A(2,\epsilon) = -(\tfrac{1}{2}J_0(\epsilon) - J_2(\epsilon)\ln 2),$$

whereupon (3.22)–(3.24) become,

$$-1 = (\tfrac{1}{2}c_2 - \ln 2)\hat{q}_0 + \hat{q}_2 c_2 - \left(\hat{q}_{-1} - \mathrm{i}\hat{q}_{-2}\frac{\partial}{\partial\epsilon}\right)J_0(\epsilon), \tag{3.25}$$

$$0 = -\hat{q}_1[1+c_2] - \mathrm{i}\left(\hat{q}_{-1} - \mathrm{i}\,\hat{q}_{-2}\frac{\partial}{\partial\epsilon}\right)J_1(\epsilon), \tag{3.26}$$

$$-\tfrac{1}{2} = \hat{q}_0[\tfrac{1}{4}c_2(1+\ln 2)] + \hat{q}_2[\tfrac{1}{2}c_2 - \ln 2] - \left(\hat{q}_{-1} - \mathrm{i}\hat{q}_{-2}\frac{\partial}{\partial\epsilon}\right)(\tfrac{1}{2}J_0(\epsilon) - J_2(\epsilon)\ln 2). \tag{3.27}$$

Similarly, using (C 1) and (C 2) in the definitions (3.12) and (3.16) of $C_2(j, \xi)$ and $D(j, \xi)$, the Kutta-condition equations (3.17) and (3.18) become

$$0 = \hat{q}_0\{1+c_2\} + 2c_2\hat{q}_1 - \mathrm{i}\left[\hat{q}_{-1} - \mathrm{i}\hat{q}_{-2}\frac{\partial}{\partial\epsilon}\right](\epsilon g(\epsilon, -1)), \tag{3.28}$$

$$0 = \hat{q}_0 4c_2 + \hat{q}_1 2c_2 + \left(\hat{q}_{-1} - \mathrm{i}\hat{q}_{-2}\frac{\partial}{\partial\epsilon}\right)\left\{\mathrm{i}\epsilon\frac{\partial}{\partial\xi}g(\epsilon, -1)\right\}, \tag{3.29}$$

where, from (B 3),

$$\left.\begin{aligned} g(\epsilon, -1) &= -[J_0(\epsilon) - \mathrm{i}J_1(\epsilon)], \\ \frac{\partial}{\partial\xi}g(\epsilon, -1) &= J_0(\epsilon) - 2\mathrm{i}\epsilon[J_0(\epsilon) - \mathrm{i}J_1(\epsilon)]. \end{aligned}\right\} \tag{3.30}$$

Equations (3.25)–(3.29) determine $\hat{q}_{-2}$, $\hat{q}_{-1}$, $\hat{q}_0$, $\hat{q}_1$, $\hat{q}_2$. In particular we find after lengthy algebraic manipulation that, correct to first order in $c_2 = (\pi s/2H)^2\tfrac{1}{6}$,

$$\hat{\alpha} = \hat{q}_{-2} = \frac{\hat{q}_0\{4c_2\mathscr{F}_1(\epsilon) - (1+c_2)\mathscr{F}_2(\epsilon)\}}{\{\mathscr{F}_2(\epsilon)\mathscr{F}'_1(\epsilon) - \mathscr{F}_1(\epsilon)\mathscr{F}'_2(\epsilon)\}}, \tag{3.31}$$

$$\hat{\beta} = \hat{q}_{-1} = -\mathrm{i}\frac{\hat{q}_0\{(1+c_2)\mathscr{F}'_2(\epsilon) - 4c_2\mathscr{F}'_1(\epsilon)\}}{\{\mathscr{F}_2(\epsilon)\mathscr{F}'_1(\epsilon) - \mathscr{F}_1(\epsilon)\mathscr{F}'_2(\epsilon)\}} \tag{3.32}$$

where primes denote differentiation with respect to ϵ and

$$\left.\begin{aligned} \mathscr{F}_1(\epsilon) &= -\epsilon g(\epsilon, -1) - 2c_2 J_1(\epsilon), \\ \mathscr{F}_2(\epsilon) &= \epsilon\frac{\partial}{\partial\xi}g(\epsilon, -1) - 2c_2 J_1(\epsilon). \end{aligned}\right\} \tag{3.33}$$

Similarly, the function $F(\epsilon)$ which determines the dependence of the zeroth-order flux q_0 on the incident acoustic pressure (see (3.21)) is given by

$$F(\epsilon) = -c_2 - \ln\left(\frac{\pi s}{2H}\right) - \frac{\mathrm{i}\left[\{(1+c_2)\mathscr{F}_2(\epsilon) - 2c_2\mathscr{F}_1(\epsilon)\}' - \{(1+c_2)\mathscr{F}_2(\epsilon) - 2c_2\mathscr{F}_1(\epsilon)\}\frac{\partial}{\partial\epsilon}\right]}{\{\mathscr{F}_2(\epsilon)\mathscr{F}'_1(\epsilon) - \mathscr{F}_1(\epsilon)\mathscr{F}'_2(\epsilon)\}} \times (J_0(\epsilon) - c_2 J_2(\epsilon)), \tag{3.34}$$

where primes again denote differentiation with respect to ϵ and the operator $\partial/\partial\epsilon$ of the second term acts on $J_0(\epsilon)-c_2 J_2(\epsilon)$.

Discarding terms which are quadratic in c_2, this expression may be written more compactly as

$$F(\epsilon) = F_0(\epsilon)-\left\{\ln\frac{\pi s}{2H}+\left(\frac{\pi s}{2H}\right)^2\frac{\hat{F}(\epsilon)}{6}\right\}, \tag{3.35}$$

where

$$F_0(\epsilon) = -\frac{\mathrm{i}[J_0(\epsilon)\,{}_0\mathscr{F}_2'(\epsilon)+{}_0\mathscr{F}_2(\epsilon)\,J_1(\epsilon)]}{[{}_0\mathscr{F}_2(\epsilon)\,{}_0\mathscr{F}_1'(\epsilon)-{}_0\mathscr{F}_1(\epsilon)\,{}_0\mathscr{F}_2'(\epsilon)]}, \tag{3.36}$$

${}_0\mathscr{F}_i = \mathscr{F}_i$ $(i = 1, 2)$ of (3.33) with $c_2 = 0$, and

$$\hat{F}(\epsilon) = 1+\frac{g_1(\epsilon)+2g_2(\epsilon)\,F_0(\epsilon)}{\{-\mathrm{i}[{}_0\mathscr{F}_2(\epsilon)\,{}_0\mathscr{F}_1'(\epsilon)-{}_0\mathscr{F}_1(\epsilon)\,{}_0\mathscr{F}_2'(\epsilon)]\}}. \tag{3.37}$$

Here (see Quinn 1985)

$$\left.\begin{aligned} g_2(\epsilon) &= J_1^2(1+2\mathrm{i}\epsilon)^2+2\epsilon^2J_0^2-6\epsilon J_1(J_0-\epsilon J_1),\\ g_1(\epsilon) &= -2J_0^2(1+4\mathrm{i}\epsilon+2\epsilon^2)+4J_1^2(3-\epsilon^2)-\frac{4J_0J_1}{\epsilon}(1-4\mathrm{i}\epsilon+\epsilon^2),\end{aligned}\right\} \tag{3.38}$$

where $J_{0,1} = J_{0,1}(\epsilon)$ and

$$\{{}_0\mathscr{F}_2(\epsilon)\,{}_0\mathscr{F}_1'(\epsilon)-{}_0\mathscr{F}_1(\epsilon)\,{}_0\mathscr{F}_2'(\epsilon)\} = \mathrm{i}\epsilon[J_1(J_0+\epsilon J_1)+\epsilon(J_0-2\mathrm{i}J_1)^2]. \tag{3.39}$$

The function $F_0(\epsilon)$ of (3.36) is independent of s/H, the ratio of the slot width to that of the duct, and is the 'zeroth-order' approximation to $F(\epsilon)$ in which the duct is infinitely wide on a hydrodynamic lengthscale U/ω. We find (Quinn 1985)

$$F_0(\epsilon) = -\frac{1}{\epsilon}\frac{\{[J_0-2\mathrm{i}\epsilon\{J_0-\mathrm{i}J_1\}]\,[J_0-\mathrm{i}\epsilon\{J_0+\mathrm{i}J_1\}]-\mathrm{i}\epsilon J_0[J_0-\mathrm{i}J_1]\}}{\{J_1(J_0+\epsilon J_1)+\epsilon(J_0-2\mathrm{i}J_1)^2\}}, \tag{3.40}$$

which agrees with Howe's (1981*b*) result. The terms in the curly brackets in (3.35) are the 'first-order' correction for small-but-finite s/H. Since the theory assumes the acoustic wavelength to be large relative to the duct height, the limit $s/H\to 0$ cannot be taken for given ϵ, M. Consequently the present problem does not reduce in all respects to the free-space problem discussed by Howe (1981*b*).

The behaviour of $F(\epsilon)$ as $\epsilon\to\infty$, particularly its imaginary part, will be relevant to the discussion of mean-flow acoustic energy exchanges of §§5, 6. Making use of the asymptotic representations of the Bessel functions (Abramowitz & Stegun 1964, p. 364) we find

$$F_0(\epsilon) \sim -\frac{\frac{1}{2}+\mathrm{i}\,\mathrm{e}^{2\mathrm{i}\epsilon}}{\frac{5}{4}-\sin 2\epsilon} \quad (\epsilon\to\infty), \tag{3.41}$$

and from (3.37)–(3.39),

$$\hat{F}(\epsilon) \sim 1+\frac{2[\frac{7}{4}-\sin 2\epsilon+\mathrm{i}\,\mathrm{e}^{2\mathrm{i}\epsilon}]}{(\frac{5}{4}-\sin 2\epsilon)^2}(\tfrac{1}{2}+\mathrm{i}\,\epsilon^{2\mathrm{i}\epsilon}) \quad (\epsilon\to\infty). \tag{3.42}$$

Use of these results in (3.35) reveals that

$$\operatorname*{Im}_{\lim\epsilon\to\infty}(F(\epsilon)) \approx -\frac{\cos 2\epsilon}{(\frac{5}{4}-\sin 2\epsilon)^2}\left\{\tfrac{5}{4}-\sin 2\epsilon+\frac{\pi s^2}{2H^2}[\tfrac{3}{4}-\sin 2\epsilon]\right\}. \tag{3.43}$$

The term in curly brackets is positive provided that $s/H < 1/2\pi^{\frac{1}{2}}$, so $\mathrm{Im}\,(F(\epsilon))$ is negative when $\cos 2\epsilon$ is positive, i.e. for small s/H there is an infinite sequence of intervals in which $\mathrm{Im}\,F(\epsilon) < 0$. A similar calculation indicates that

$$F(\epsilon) \approx \left[-\ln\left(\frac{\pi s}{2H}\right)-\frac{2}{3\epsilon^2}\left\{1-\frac{1}{2}\left(\frac{\pi s}{2H}\right)^2\right\}\right]+\mathrm{i}\frac{16}{9\epsilon}\left\{1+\left(\frac{\pi s}{2H}\right)^2\frac{5}{12}\right\} \quad (\epsilon \ll 1). \tag{3.44}$$

4. Case II: the effect of vorticity ejection modelled by displacement-thickness waves

When displacement-thickness waves are included in the theoretical model the total flux, $Q = q_0 + q_h$, may be derived by a simple extension of the analysis of §3.1. An additional equation for the unknown amplitude h of the displacement waves is obtained by requiring ζ to remain finite at the slot trailing edge. In §3 ζ satisfied the Kutta condition at the leading edge but had an inverse square-root singularity at the trailing edge, i.e.

$$\lim_{\xi\to+1-0}\zeta(\xi) = O\left[\frac{1}{(1-\xi)^{\frac{1}{2}}}\right],$$

as in the analogous problem treated by Howe (1981*b*).

Consider (2.18). The logarithmic kernel on the left-hand side is expanded as in §3 by use of (2.19) and (2.20). The integral on the right-hand side represents the influence of the displacement waves. It cannot be expanded as in (2.19), since that would require that $|\xi-\eta|(s/2H) < 1$, whereas the integration variable η varies from $+1$ to ∞. Let $\Omega(\sigma, \eta)$ be defined by

$$\Omega(\sigma, \eta) = \int_{+1}^{\infty} \mathrm{e}^{\mathrm{i}\sigma\tau} \ln\left\{\frac{\sinh\{(\tau-\eta)\,\pi s/2H\}}{(\pi s/2H)}\right\} \mathrm{d}\tau. \tag{4.1}$$

The analogue of the integral equation (3.1) is accordingly

$$\int_{-1}^{+1} \zeta(\eta) \ln|\xi-\eta|\,\mathrm{d}\eta = \chi(\xi),$$

where

$$\chi(\xi) = \chi_0(\xi)+\chi_1(\xi)-h\Omega(\sigma, \xi), \tag{4.2}$$

and χ_0 is given by (3.2) with q_0 replaced by Q, the total flux, and χ_1 is defined by (3.3). The formal solution (3.5) is now subject to the boundary conditions (3.9), together with the additional requirement that $\zeta(+1-0) < \infty$, which is satisfied provided that

$$\lim_{\xi\to+1-0}\{q_0+\Theta_1(\chi, \xi)\} = 0. \tag{4.3}$$

The calculation proceeds exactly as in §3.1; indeed one obtains (3.11) for $\zeta(\xi)$ with just two modifications: E is defined as in (3.13) but with q_0 replaced by Q; and the following linear functional, $h[\Theta_0(\Omega)-\ln 2\Theta_1(\Omega, \xi)]$, generated by the term in $\Omega(\sigma, \xi)$ on the right of (4.2), must be added to the expression within the curly brackets of (3.11). As before the fluxes q_n are normalized with respect to E, and h is denoted by q_{-3}, and one obtains the system of linear equations (3.14), (3.17) and (3.18) but with the right-hand sides supplemented by terms in $\hat{q}_{-3} = \hat{h}$. These are, respectively,

$$\left.\begin{aligned} &\hat{q}_{-3}\{\Theta_0(\Omega)\,a_m-\ln 2\,\omega_m(\sigma)\}, \quad \hat{q}_{-3}\{-\Theta_1(\Omega, -1)\}, \\ &\hat{q}_{-3}\left\{\frac{\partial}{\partial\xi}\Theta_1(\Omega, -1)\right\}, \end{aligned}\right\} \tag{4.4}$$

where

$$\omega_m(\sigma) = \frac{1}{\pi}\int_{-1}^{+1} \frac{\xi^m \Theta_1(\Omega, \xi)}{(1-\xi^2)^{\frac{1}{2}}}\,\mathrm{d}\xi. \tag{4.5}$$

The extra equation arising from condition (4.3) has the form

$$0 = \hat{q}_0 - \sum_{r=0}^{2N-1} \hat{q}_r C_2(r, +1) - \left\{\hat{q}_{-1} - \mathrm{i}\hat{q}_{-2}\frac{\partial}{\partial\epsilon}\right\}(\mathrm{i}\epsilon g(\epsilon, +1)) - \hat{q}_{-3}\Theta_1(\Omega, +1). \tag{4.6}$$

The additional integrals $\Theta_0(\Omega)$, $\Theta_1(\Omega, \xi)$ and $\omega_m(\sigma)$ of (4.5) are computed in Appendix D by introducing the following partition of $\Omega(\sigma, \eta)$ of (4.1):

$$\left.\begin{aligned} \Omega(\sigma, \eta) &= \Omega_1(\sigma, \eta) + \Omega_2(\sigma, \eta), \\ \text{where} \qquad \Omega_1(\sigma, \eta) &= \int_{+1}^{\infty} \mathrm{e}^{\mathrm{i}\sigma\tau} \ln(\tau - \eta)\,\mathrm{d}\tau, \\ \text{and} \qquad \Omega_2(\sigma, \eta) &= \int_{+1}^{\infty} \mathrm{e}^{\mathrm{i}\sigma\tau} \ln\left\{\frac{\sinh([\tau-\eta]\pi s/2H)}{(\tau-\eta)\pi s/2H}\right\}\mathrm{d}\tau. \end{aligned}\right\} \tag{4.7}$$

The solution of the $(2N+4)$ linear equations yields a relationship between the total flux Q and $p_0\pi/2\rho_0 U^2\epsilon^2$ in terms of the function $F(\epsilon)$, which is now defined by

$$Q\{\ln 2 - \tfrac{1}{2}\pi[c_+ + c_-] + F(\epsilon)\} = \frac{p_0\pi}{2\rho_0 U^2\epsilon^2}. \tag{4.8}$$

As before, $F(\epsilon)$ is ultimately a periodic function of ϵ with period π when ϵ is large. This can be deduced from the system of linear equations in the manner discussed in §3.1.

The behaviour of the displacement ζ at the trailing edge of the slot will now be examined. From (3.5), (3.8), (4.2) and (4.4),

$$\begin{aligned} \lim_{\xi\to+1-0}\zeta(\xi) &= \lim_{\phi\to 0}\left\{\frac{q_0 + \Theta_1(\chi, \cos\phi)}{\pi\sin\phi}\right\} \\ &= \lim_{\phi\to 0}\left\{\frac{1}{\pi}\frac{\partial}{\partial\phi}\Theta_1(\chi, \cos\phi)\right\} \\ &= \lim_{\phi\to 0}\frac{1}{\pi}\frac{\partial}{\partial\phi}\{\Theta_1(\chi_0, \cos\phi) + \Theta_1(\chi_1, \cos\phi) - h\Theta_1(\Omega, \cos\phi)\}. \end{aligned} \tag{4.9}$$

Equations (C 2), (C 3) of Appendix C reveal that χ_1 can make no contribution to (4.9). Similarly it follows from Appendix D that the contribution from the component Ω_2 of Ω, (4.7), will be of the form

$$g(\sigma, \cos\phi) \times \{\text{polynomial of degree } 2N \text{ in } \cos\phi\}.$$

The functionals $\Theta_1(\chi_0, \xi)$, $\Theta_1(\Omega_1, \xi)$ are given in (B 2), (D 3), respectively, and (4.9) reduces to

$$\lim_{\xi\to+1-0}\zeta(\xi) = \lim_{\phi\to 0}\frac{\partial}{\partial\phi}\left\{\sin\phi\sum_{n=1}^{\infty}\beta_n\sin n\phi\right\}, \tag{4.10}$$

where

$$\beta_n = \frac{2(\mathrm{i})^n}{\pi}\left\{h\,\mathrm{e}^{\mathrm{i}\sigma}I_n + \left(\beta - \mathrm{i}\alpha\frac{\partial}{\partial\epsilon}\right)\mathrm{i}\epsilon J_n(\epsilon) + \gamma h J_n(\sigma)\right\}. \tag{4.11}$$

Here γ is a constant and the I_n are defined by (D 4). The calculation proceeds as in §4 of Howe (1981*b*). For $n \gg |\sigma|$ (see Howe 1981*b*, A 12),

$$I_n \approx \frac{(-\mathrm{i})^n}{n}\left\{1+\frac{\mathrm{i}\sigma}{n^2-1}+\frac{1\times 3(\mathrm{i}\sigma)^2}{(n^2-1)\,(n^2-2^2)}+\ldots\right\} \tag{4.12}$$

and since $J_n(z) \approx (\frac{1}{2}z)^n\, 1/n!$ for large n we deduce that

$$\beta_n \approx \bar{\beta}_n = \frac{2h}{\pi n}\,\mathrm{e}^{\mathrm{i}\sigma} \quad (n\to\infty). \tag{4.13}$$

Consequently the series (4.10) does not converge uniformly in $(0, \pi)$. The non-uniformity is avoided by writing (4.10) as follows:

$$\lim_{\xi\to+1-0}\zeta(\xi) = \lim_{\phi\to 0}\frac{\partial}{\partial\phi}\left\{\sin\phi\left[\sum_{n=1}^{\infty}(\beta_n-\bar{\beta}_n)\sin n\phi+\sum_{n=1}^{\infty}\bar{\beta}_n\sin n\phi\right]\right\},$$

where the second series can be summed (Gradshteyn & Ryzhik 1980, p. 38). This leads to

$$\begin{aligned}\lim_{\xi\to+1-0}\zeta(\xi) &= \lim_{\phi\to 0}\frac{\partial}{\partial\phi}\left\{\sin\phi\left[h\,\mathrm{e}^{\mathrm{i}\sigma}\left(1-\frac{\phi}{\pi}\right)+\sum_{n=1}^{\infty}(\beta_n-\bar{\beta}_n)\sin n\phi\right]\right\}\\ &= h\,\mathrm{e}^{\mathrm{i}\sigma}+\lim_{\phi\to 0}\frac{\partial}{\partial\phi}\left\{\sin\phi\sum_{n=1}^{\infty}(\beta_n-\bar{\beta}_n)\sin n\phi\right\}.\end{aligned} \tag{4.14}$$

The contribution from the remaining series vanishes since (cf. (4.12)) the coefficients $\beta_n-\bar{\beta}_n = O(1/n^3)$ $(n\to\infty)$. Thus

$$\lim_{\xi\to+1-0}\zeta(\xi) = h\,\mathrm{e}^{\mathrm{i}\sigma}, \tag{4.15}$$

implying that ζ merges continuously with the displacement-thickness waves at the trailing edge.

Equation (4.15) is valid when the duct is infinitely wide $(s/H\to 0)$ (Howe 1981*b*). In this same limit the formula for $F(\epsilon)$, $F_0(\epsilon)$, is given by Howe's equation (3.9) from which it can be shown that

$$\lim_{\epsilon\to\infty}F_0(\epsilon) \sim -\frac{(1-\epsilon/\sigma)\{\frac{1}{2}(1-\epsilon/\sigma)+\mathrm{i}\,\mathrm{e}^{2\mathrm{i}\epsilon}\}}{\frac{1}{4}(1-\epsilon/\sigma)^2+1-(1-\epsilon/\sigma)\sin 2\epsilon}, \tag{4.16}$$

this asymptotic form being a correction to Howe's equation (3.13). For $s \ll H$, $F(\epsilon)$ is related to $F_0(\epsilon)$ by an equation of the form (3.34), i.e.

$$F(\epsilon)) = F_0(\epsilon)-\ln\frac{\pi s}{2H}+O\left(\left(\frac{\pi s}{2H}\right)^2\right) \quad (s \ll H).$$

5. Mean-flow/acoustic energy exchanges

At large distances upstream or downstream of the slot the acoustic fields behave as plane waves. This is easily seen from (2.5) when use is made of the asymptotic forms of the Green functions $G_\pm$ given by (A 2)–(A 4). Consider the plane control surfaces $S_i^\pm$ $(i = 1, 2)$ of figure 2, which are normal to both the plate and the mean flow at $x_1 = \pm l$, where $2H/\pi < |l| < 1/k$. Let the reflected waves at $S_2^\pm$ have complex amplitudes $\phi_0 R_+$, $\phi_0 R_-$ respectively, and let the corresponding transmitted-wave amplitudes be denoted by $\phi_0 T_+$, $\phi_0 T_-$ where ϕ_0 is the amplitude of the incident wave ϕ_1^+ of (2.1).

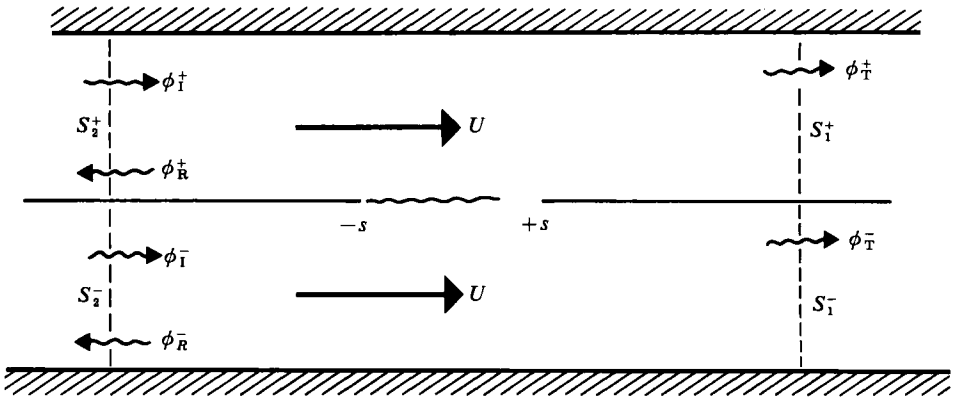

FIGURE 2. The form of the acoustic field at $x_1 = \pm l$, $2H/\pi \ll l \ll 1/k$.

When $M \ll 1$, so that convection of sound by the mean flow can be neglected, we find from (2.5), (2.6) and (A 2)–(A 4) that the total perturbation pressure in $x_2 > 0$ is given to leading order by

$$\frac{p_+}{\rho_0} \approx \omega^2\left\{-\frac{\mathrm{i}}{2kH}\,\mathrm{e}^{\mathrm{i}k|x_1|}\right\}\int_{-s}^{+\infty} Z_+(y)\,\mathrm{d}y + \frac{p_0^+}{\rho_0}$$

$$= \mathrm{i}\omega\{\phi_0 R_+\,\mathrm{e}^{\mathrm{i}k|x_1|}\} + \frac{p_0^+}{\rho_0} \tag{5.1}$$

for $2H/\pi < |x_1|$, where

$$\phi_0 R_+ = -\frac{\omega s^2 Q}{2kH}, \quad \frac{p_0^+}{\rho_0} \approx \mathrm{i}\omega\phi_0\,\mathrm{e}^{\mathrm{i}kx_1} \quad (M \ll 1). \tag{5.2}$$

The corresponding total perturbation potential is obtained from the linearized Bernoulli equation

$$\phi_+ \approx \phi_0 R_+\,\mathrm{e}^{\mathrm{i}k|x_1|} + \phi_0\,\mathrm{e}^{\mathrm{i}kx_1} \quad (M \ll 1). \tag{5.3}$$

For $2H/\pi < |x_1| < 1/k$, (5.1) and (5.2) may be approximated by

$$\frac{p_+}{\rho_0} \approx \mathrm{i}\omega\phi_0(R_+ + 1) = \mathrm{i}\omega\phi_0 T_+. \tag{5.4}$$

Similarly from (5.3), $\partial\phi_+/\partial x_1$ satisfies

$$\frac{\partial\phi_+}{\partial x_1} \approx \mathrm{i}k\phi_0\{\pm R_+ + 1\} \quad (x_1 \gtrless 0). \tag{5.5}$$

The total perturbation pressure and potential in $x_2 < 0$ are calculated from (2.5), (2.7) and (A 2)–(A 4) enabling the following results to be derived as in (5.1)–(5.5) for $2H/\pi < |x_1| < 1/k$:

$$\left.\begin{aligned} \frac{p_-}{\rho_0} &\approx \mathrm{i}\omega\phi_0[R_-\,\mathrm{e}^{\mathrm{i}k|x_1|} + \mathrm{e}^{\mathrm{i}(kx_1-\theta)}] \\ &\approx \mathrm{i}\omega\phi_0(R_- + \mathrm{e}^{-\mathrm{i}\theta}) = \mathrm{i}\omega\phi_0 T_-, \\ \phi_- &\approx \phi_0 R_-\,\mathrm{e}^{\mathrm{i}k|x_1|} + \phi_0\,\mathrm{e}^{\mathrm{i}(kx_1-\theta)}, \end{aligned}\right\} \tag{5.6}$$

$$\frac{\partial\phi_-}{\partial x_1} \approx \mathrm{i}k\phi_0\{\pm R_- + \mathrm{e}^{-\mathrm{i}\theta}\} \quad (x_1 \gtrless 0), \tag{5.7}$$

where

$$R_- = +\frac{\omega s^2 Q}{2kH}. \tag{5.8}$$

The time-averaged acoustic-power flux through S_1^+, $\Pi_{S_1^+}$ say, is given by

$$\Pi_{S_1^+} = \frac{1}{4}\int_0^H \left\{p_+ \frac{\partial \phi_+^*}{\partial x_1} + \text{c.c.}\right\} \mathrm{d}x_2 \quad (x_1 = l), \tag{5.9}$$

where mean-flow convection has again been neglected, the asterisk denotes the complex-conjugate, and c.c. denotes the complex-conjugate of the preceding expression.

Use of (5.4) and (5.5) in (5.9) show that

$$\Pi_{S_1^+} = \frac{\rho_0 \omega k H}{2} |\phi_0|^2 |T_+|^2. \tag{5.10}$$

Similarly the corresponding power fluxes $\Pi_{S_2^\pm}$, $\Pi_{S_1^-}$ through $S_2\pm$, S_1- respectively, are found to be

$$\Pi_{S_2+} = \tfrac{1}{2}\rho_0 \omega k H |\phi_0|^2 (1 - |R_+|^2), \tag{5.11}$$

$$\Pi_{S_1-} = \tfrac{1}{2}\rho_0 \omega k H |\phi_0|^2 |T_-|^2, \tag{5.12}$$

$$\Pi_{S_2-} = \tfrac{1}{2}\rho_0 \omega k H (1 - |R_-|^2), \tag{5.13}$$

where, from (5.4) and (5.6),

$$T_+ = 1 + R_+, \quad T_- = \mathrm{e}^{-\mathrm{i}\theta} + R_-. \tag{5.14}$$

The total transmitted power, Π_+ say, is therefore given by

$$\Pi_+ = \Pi_{S_1+} + \Pi_{S_1-} = \tfrac{1}{2}\rho_0 \omega k H |\phi_0|^2 [|T_+|^2 + |T_-|^2] \tag{5.15}$$

and the total incident flux, Π_- say, by

$$\Pi_- = \Pi_{S_2+} + \Pi_{S_2-} = \tfrac{1}{2}\rho_0 \omega k H |\phi_0|^2 [2 - |R_+|^2 - |R_-|^2]. \tag{5.16}$$

Hence the total acoustic power produced through the mean flow–acoustic interaction at the slot Π is

$$\Pi = \Pi_+ - \Pi_- = \tfrac{1}{2}\rho_0 \omega k H |\phi_0|^2 [|T_+|^2 + |T_-|^2 - 2 + |R_+|^2 + |R_-|^2]. \tag{5.17}$$

Noting that $R_- = -R_+$ from (5.2) and (5.8) and using (5.14) we find that

$$\Pi = \tfrac{1}{2}\rho_0 \omega k H |\phi_0|^2 [2|R_+|^2 + R_+\{1 - \mathrm{e}^{+\mathrm{i}\theta}\} + \text{c.c.}]$$

and thence from (5.2) that

$$\begin{aligned} \Pi &= \tfrac{1}{2}\rho_0 \omega k H \left[\frac{2\omega^2 s^4 |Q|^2}{4k^2 H^2} - \frac{\omega s^2 Q}{2kH}\{\phi_0^*(1 - \mathrm{e}^{\mathrm{i}\theta})\} + \text{c.c.}\right] \\ &= \rho_0 \omega^3 s^4 \left[\frac{|Q|^2}{4kH} - \mathrm{i}\frac{Q}{2\pi}\frac{\{\pi p_0/\rho_0\}^*}{\{2U^2\epsilon^2\}} + \text{c.c.}\right], \end{aligned} \tag{5.18}$$

since from (2.11), (2.17), we have, respectively,

$$\left.\begin{aligned} \frac{p_0}{\rho_0} = \frac{p_0^+ - p_0^-}{\rho_0} &= \mathrm{i}\omega\phi_0(1 - \mathrm{e}^{-\mathrm{i}\theta}) \\ U^2\epsilon^2 &= \omega^2 s^2. \end{aligned}\right\} \tag{5.19}$$

Finally, using (4.8) with the aid of (A 4) we reduce (5.18) to the compact form

$$\Pi = -\frac{\rho_0 \omega^3 s^4 |Q|^2}{\pi} \operatorname{Im} F(\epsilon). \tag{5.20}$$

Since by hypothesis the radian frequency ω is positive, this result implies that acoustic energy is absorbed at the slot when $\operatorname{Im} F(\epsilon) > 0$, and is generated when $\operatorname{Im} F(\epsilon) < 0$.

The flux Π_- of (5.16), expressed in terms of Q from (5.2) and (5.8), is

$$\Pi_- = \rho_0 \omega k H |\phi_0|^2 \left\{1 - \frac{|\omega s^2 (Q/\phi_0)|^2}{4k^2 H^2}\right\}. \tag{5.21}$$

Normalizing the transmitted flux Π_+ by Π_-, the total incident flux yields, with use of (5.17), (5.20) and (5.21),

$$\frac{\Pi_+}{\Pi_-} = 1 - \frac{|\omega s^2 (Q/\phi_0)|^2 \, (\operatorname{Im} F(\epsilon)/\pi k H)}{\{1 - |\omega s^2 (Q/\phi_0)|^2 / 4k^2 H^2\}}. \tag{5.22}$$

From (5.19), (A 4) and the definition (4.8) of $F(\epsilon)$ we find

$$\frac{\omega s^2 Q}{\phi_0} = \frac{\pi \mathrm{i}(1 - \mathrm{e}^{-\mathrm{i}\theta})}{2\{F(\epsilon) + \pi \mathrm{i}/2kH\}} \tag{5.23}$$

and substitution into (5.22) gives

$$\frac{\Pi_+}{\Pi_-} = 1 - \frac{\pi(1 - \cos\theta)\,(\operatorname{Im} F(\epsilon)/2kH)}{\left\{\left|F(\epsilon) + \dfrac{\pi \mathrm{i}}{2kH}\right|^2 - \dfrac{\pi^2 (1 - \cos\theta)}{8k^2 H^2}\right\}}. \tag{5.24}$$

In the absence of an incident wave in the region $x_2 < 0$ the total transmitted and incident power fluxes are easily deduced from (5.14)–(5.16). Equation (5.15) remains valid, but in (5.14) we set

$$T_- = R_-$$

and subtract from (5.16) the power flux $\Pi_{\mathrm{I}}^- \approx \frac{1}{2}\rho_0 \omega k H |\phi_0|^2$ associated with the wave ϕ_{I}^- of (2.1). Consequently (5.20) is still true, but now (5.23) becomes

$$\frac{\omega s^2 Q}{\phi_0} = \frac{\frac{1}{2}\pi \mathrm{i}}{F(\epsilon) + \pi \mathrm{i}/2kH} \tag{5.25}$$

and we find that the normalized flux Π_+/Π_- is given by (5.24) with the phase difference θ equal to $\frac{1}{2}\pi$.

It is of interest to examine the possibility of there being a zero or negative net flux of acoustic power through the upstream control surfaces S_2^+, S_2^-, i.e. $\Pi_- \leqslant 0$. According to equations (5.21), (5.23),

$$\left\{|F(\epsilon)|^2 + \frac{\pi^2}{8k^2 H^2}(1 + \cos\theta)\right\} + \frac{\operatorname{Im} F(\epsilon)}{2kH} \gtrless 0 \quad \text{for} \quad \Pi_- \gtrless 0. \tag{5.26}$$

Hence, Π_- is certainly positive for $\operatorname{Im} F(\epsilon) > 0$, when acoustic energy is absorbed at the slot, but may possibly become negative when there is a net production of acoustic energy at the slot ($\operatorname{Im} F(\epsilon) < 0$).

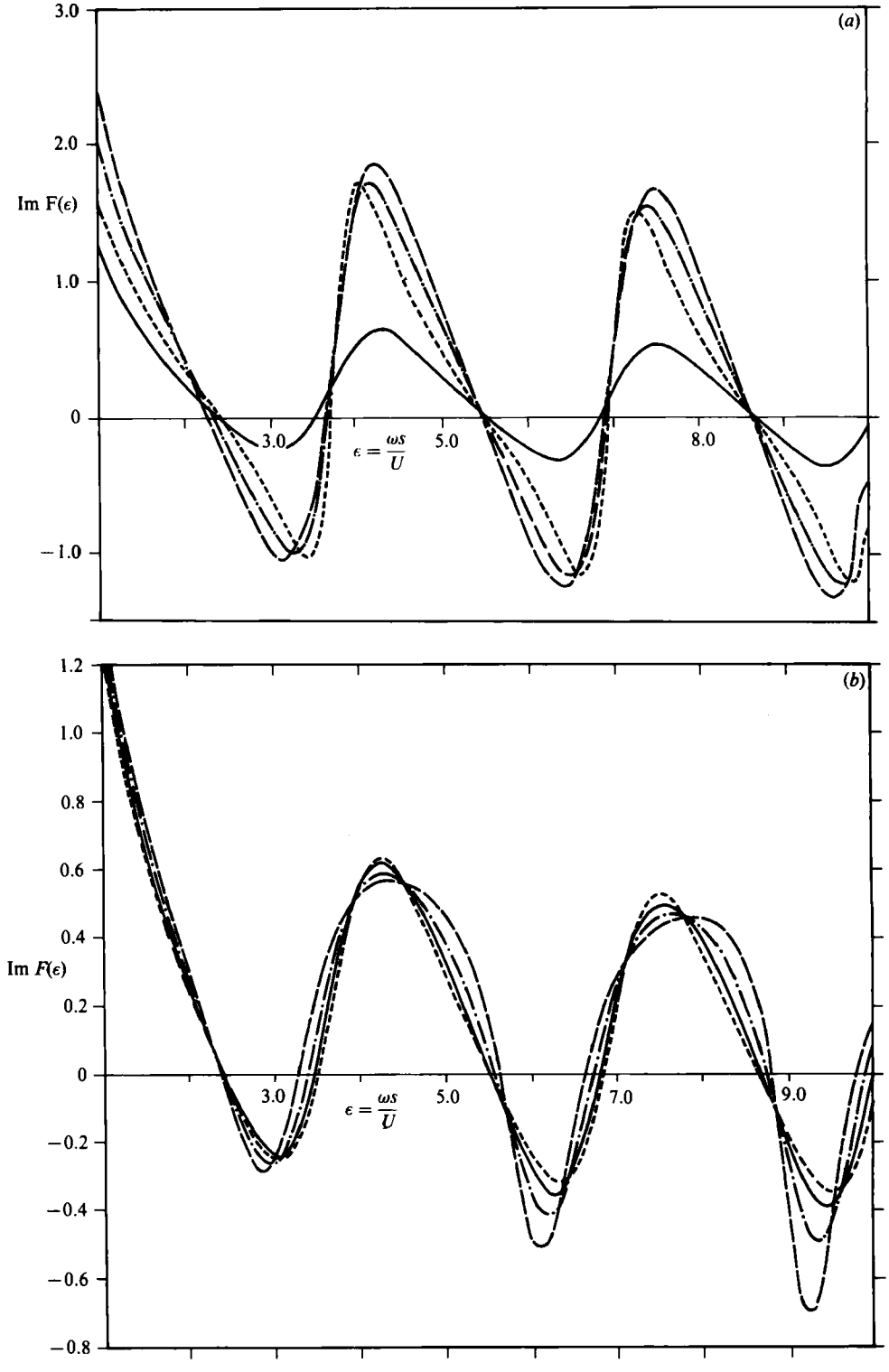

FIGURE 3. The behaviour of Im $F(\epsilon)$ for $\epsilon > 1$: -----, $s/H = 0$; ——, 0.3; –·–·, 0.5; – – –, 0.7. (*a*) Case I with the zeroth-order solution of Case II, (——, $s/H = 0$ of Case II). (*b*) Case II.

6. Numerical results

6.1. *Production/absorption of acoustic energy at the slot*

Equations (3.21) and (4.8) are equivalent definitions of $F(\epsilon)$, since in the absence of displacement waves (Case I) the total flux Q is equal to q_0. The effect of the displacement-thickness fluctuations cannot be assessed until their wavenumber $\sigma = \omega s/V$ is specified in terms of the Strouhal number $\epsilon = \omega s/U$. In the following we take $\sigma = \frac{5}{3}\epsilon$, which is assumed to be representative of typical large-scale boundary-layer disturbances convecting at about 60 % of the mainstream velocity (cf. Bull 1967; Black 1970).

The behaviour of $\operatorname{Im} F(\epsilon)$ for $\epsilon > 1$ for the general Case II, in which allowance is made for the influence of displacement-thickness fluctuations, is illustrated in figure 3(*b*), for different values of s/H. The results confirm our earlier conclusion (§§3, 4) that $F(\epsilon)$ becomes periodic when ϵ is large, and that there exists an infinite set of equally spaced frequency intervals of length π within which $\operatorname{Im} F(\epsilon) < 0$ and acoustic energy is extracted from the mean flow in accordance with (5.20). The corresponding results for Case I are shown in figure 3(*a*), together with the 'zeroth'-order solution, $s/H = 0$, of Case II for comparison. It can be seen that the position of frequency intervals in which $\operatorname{Im} F(\epsilon) < 0$ does not vary significantly between the two cases, but that the predictions of the magnitude of $\operatorname{Im} F(\epsilon)$ are very different.

To examine energy exchanges at the slot the rate of production of acoustic energy Π, given by (5.20), is normalized with respect to the *total* incident power flux $\Pi_1 = \rho_0 \omega k H |\phi_0|^2$, say, associated with the waves ϕ_{I}^+, ϕ_{I}^-. Using (5.20) and (5.23) we have

$$-\frac{\Pi}{\Pi_1} = \frac{\pi(1-\cos\theta)\operatorname{Im} F(\epsilon)}{2kH|F(\epsilon)+\pi \mathrm{i}/2kH|^2}. \tag{6.1}$$

This is plotted as a function of $ks = \omega s/c$ for different values of s/H in figures 4(*a*, *b*) and 5(*a*, *b*) respectively for Cases I and II, when the phase difference θ between the incident waves is $\frac{1}{2}\pi$ and $M = 0.05, 0.1$. A range $0 < ks < 0.24$ is chosen to satisfy the requirement $ks \ll 1$ while retaining some of the more interesting features of the predictions (see figures 4*a*, 5*a*). Acoustic energy is being absorbed/produced at the slot according as $-\Pi/\Pi_1 \gtrless 0$.

Figures 3(*a*, *b*) indicate that $\operatorname{Im} F(\epsilon)$ is positive for ϵ less than about 2.4. Consequently, as the Mach number increases from 0.05 to 0.1, the range of $ks(= \epsilon M)$ in which $\operatorname{Im} F(\epsilon) > 0$ and (cf. (5.20)) there is attenuation, increases proportionately. That behaviour is demonstrated in figures 4(*a*, *b*) and 5(*a*, *b*) which also show that when $0(M) \leqslant ks < 0.24M$ more of the incident sound is absorbed as M increases, but the attenuation is decreased as the frequency or s/H increase. The differences in the predictions of Cases I and II are most marked when ϵ is very small ($ks \ll M$) and when acoustic energy is being produced at the slot ($ks > 2.4M$).

(i) $ks \ll M$

This range of ks corresponds to $\epsilon = ks/M \ll 1$. Figures 4(*a*, *b*) of Case I predict that $-\Pi/\Pi_1$ decreases rapidly to zero as $ks \to 0$. By contrast, the results of figures 5(*a*, *b*) imply that the influence of the ejected vorticity is to make $-\Pi/\Pi_1$ tend to a finite non-zero limit as $\epsilon \to 0$. This difference can be explained, at least for small s/H, by consideration of the relative magnitude of the real and imaginary parts of $F(\epsilon)$ as $\epsilon \to 0$.

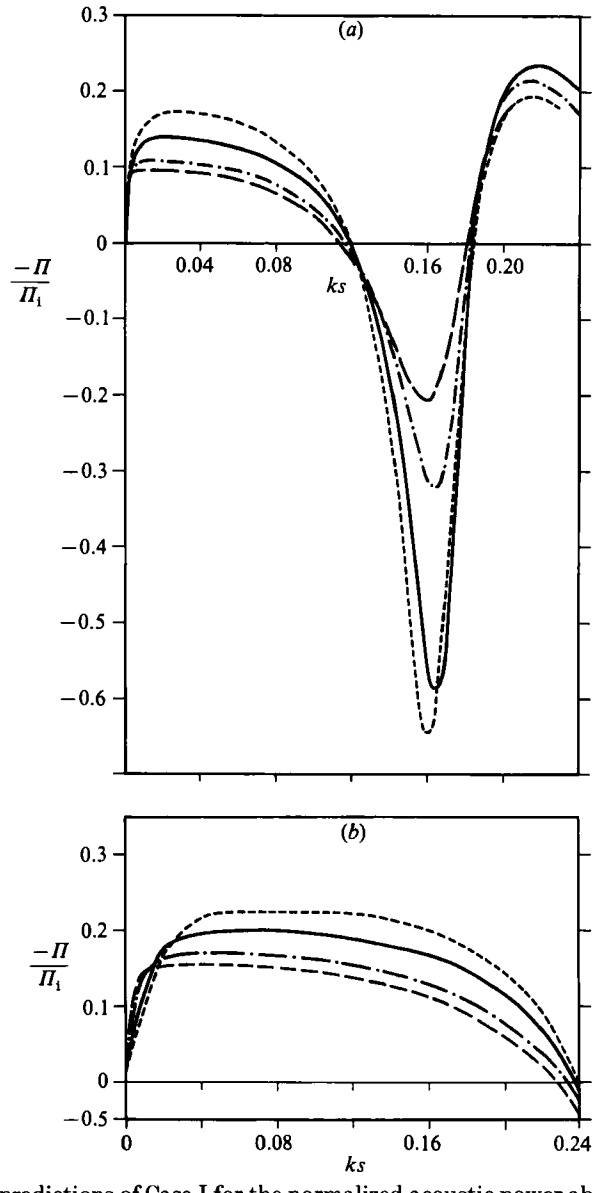

FIGURE 4. The predictions of Case I for the normalized acoustic power absorbed at the slot, $-\Pi/\Pi_1$ of (6.1), as a function of ks with: -----, $s/H = 0.2$, and $s/H = 0.3$, 0.5, 0.7 as indicated for figure 3. (*a*) $M = 0.05$, (*b*) $M = 0.1$.

For Case I, (3.44) gives

$$\mathrm{Im}\, F(\epsilon) \approx \frac{16}{9\epsilon}, \quad \mathrm{Re}\, F(\epsilon) \approx -\frac{2}{3\epsilon^2} \quad (\epsilon \to 0, \quad s \ll H),$$

which on substitution in (6.1) (with $\epsilon/kH = (s/H)/M$) yields

$$-\frac{\Pi}{\Pi_1} \approx \frac{8\pi}{9} \frac{(1-\cos\theta)\,[(s/H)/M]\,\epsilon^2}{\left\{\frac{4}{9} + \epsilon^2\left(\frac{16}{9} + \frac{1}{2}\pi\frac{(s/H)}{M}\right)\right\}} \sim 0 \quad (\epsilon \to 0, \quad s \ll H). \tag{6.2}$$

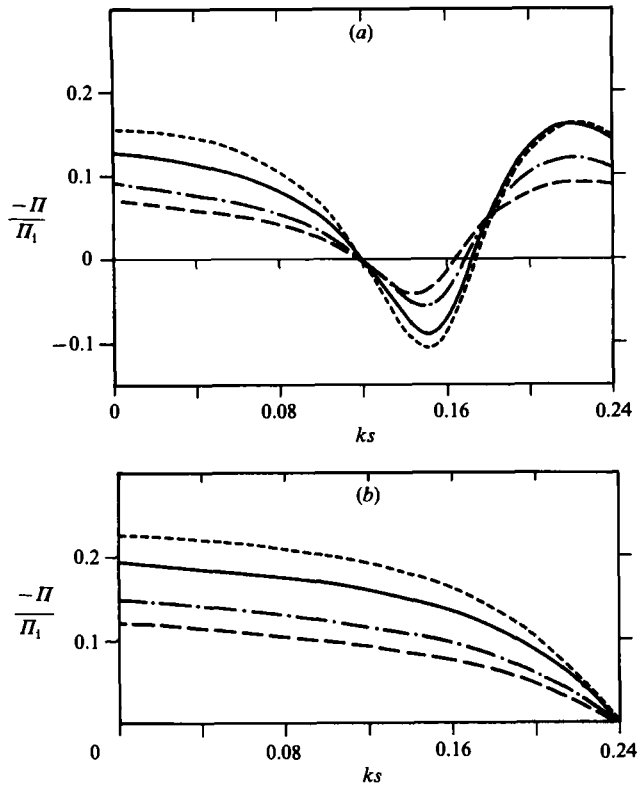

FIGURE 5. As figure 4, but for Case II.

On the other hand, in Case II and for $s \ll H$ (cf. Howe 1981*b*)

$$F(\epsilon) \sim \frac{\mathrm{i}\sigma}{\epsilon^2} = \frac{5\mathrm{i}}{3\epsilon} \quad (\epsilon \to 0, \quad s \ll H), \tag{6.3}$$

which implies say, from (6.1),

$$-\frac{\Pi}{\Pi_i} \approx \frac{5\pi}{6} \frac{[(s/H)/M](1-\cos\theta)}{\left\{\frac{5}{3}+\frac{\pi s/H}{2M}\right\}^2} = \Pi_0, \quad \text{for} \quad ks \ll M, \quad ks \ll \frac{s}{H} \ll 1. \tag{6.4}$$

The limiting value Π_0 is a maximum of 0.5 when $s/H = M/(0.3\pi)$ and $\theta = \pi$.

(ii) $ks \gg M$.

For $M \leqslant 0.05$ the Strouhal number ϵ exceeds $O(1)$ over most of the interval $0 < ks < 0.24$, and the power flux $-\Pi/\Pi_1$ oscillates, taking positive/negative values corresponding to absorption/production of acoustic energy.

The onset of oscillatory behaviour is evident in figure 4(*a*) (Case I). Comparison with figure 5(*a*) (Case II) reveals that neglecting the influence of ejected vorticity results in much larger predictions of the amount of acoustic energy produced at the slot, but in both Cases I and II the production/absorption tends to be reduced as s/H increases.

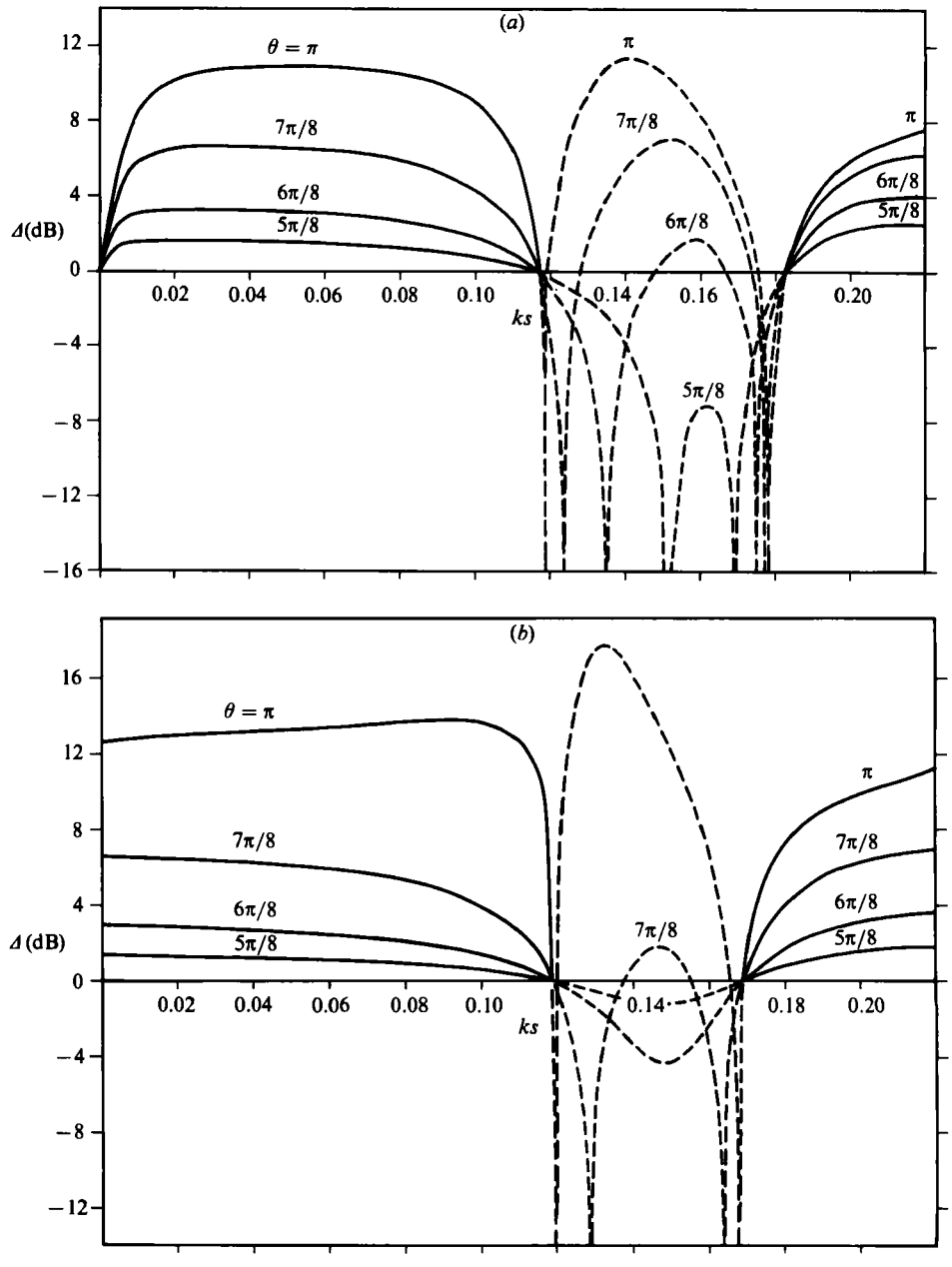

FIGURE 6. Plot of Δ, (6.5), in dB against ks for various phase angles θ and $M = 0.05$, $s/H = 0.5$. Absorption/production of acoustic energy at the slot is indicated by solid/dashed curves respectively. (*a*) Case I, (*b*) Case II.

6.2. *Application to the experiment*

The experiment referred to in the Introduction will determine the ratio of the transmitted flux to the net incident flux (incident plus reflected), i.e. the quantity Π_+/Π_- of (5.24). We define a transmission factor Δ by

$$\Delta = -10 \log_{10}(|\Pi_+/\Pi_-|) \text{ dB}, \tag{6.5}$$

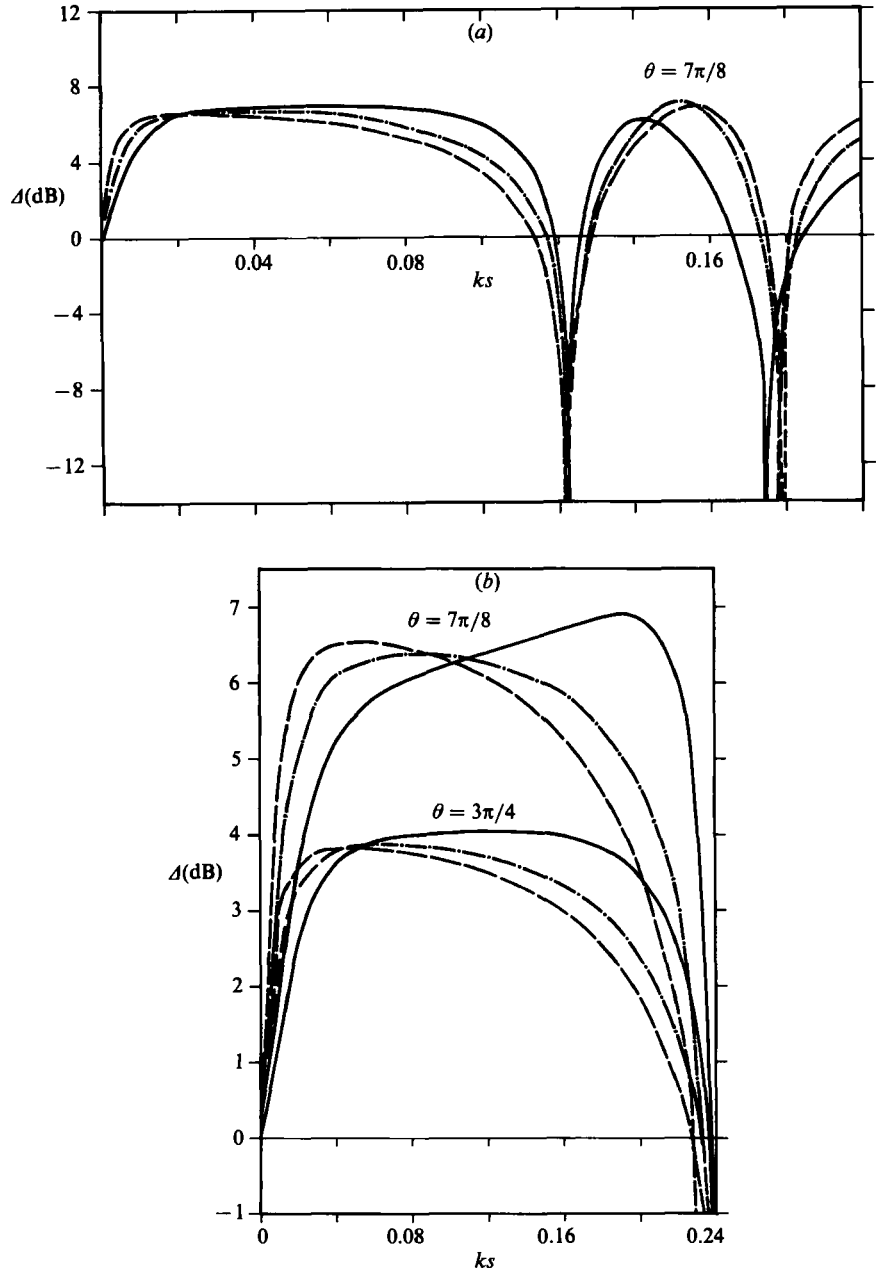

FIGURE 7. (Case I). Δ of (6.5) in dB as a function of ks for various ratios s/H (the curves being indicated as in figures 4 and 5) and values of θ. (*a*) $M = 0.05$. (*b*) $M = 0.1$.

the modulus of the ratio being taken since (cf. (5.26)) Π_+/Π_- can be negative when there is a net production of acoustic energy. From (5.24) the dependence of Δ on the phase angle θ appears in both the energy produced at the slot as in (6.1), and the back-scattered energy of Π_-. In figure 6(*a*) (Case I, $s/H = 0.5$) and 6(*b*) (Case II, $s/H = 0.5$), Δ is plotted as a function of ks for various phase angles θ and $M = 0.05$.

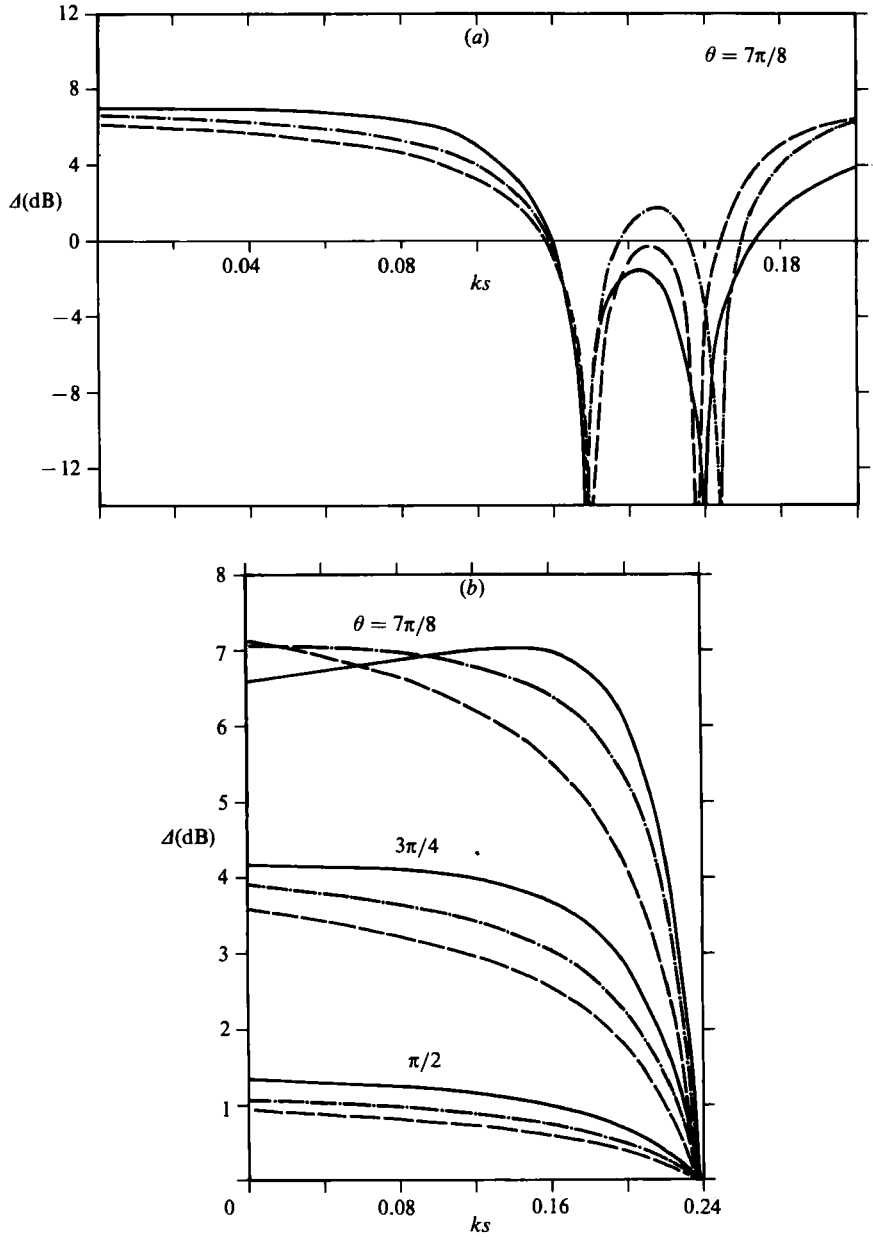

FIGURE 8. As figure 7, but for Case II.

Solid lines indicate absorption of energy at the slot while dashed lines indicate that acoustic energy is produced. From (6.5)

$$\Delta \gtrless 0 \quad \text{as} \quad |\Pi_+/\Pi_-| \lesseqgtr 1.$$

Figure 6(*a*) (Case I) shows that when the slot is producing acoustic energy, Δ can become singular, i.e. $\Delta \sim -\infty$. This corresponds to zeros of the flux Π_- which occur when the energy flux of the incident waves ϕ_{I}^+, ϕ_{I}^-, viz. Π_{I}, is exactly balanced by that backscattered from the flow/acoustic interaction at the slot. Two zeros of Π_-

are evident for each value θ given in figure 6 (*a*), the region between them corresponding to $\Pi_- < 0$. It can be seen that increasing the phase angle θ produces larger values of Δ, and increases the frequency range in which $\Pi_- < 0$. This is to be expected, in that the applied pressure difference $p_0 = p_0^+ - p_0^-$, due to the incident waves of (2.11), which forces the motion of the vortex sheet within the slot, increases as θ increases from 0 to π. The magnitude of the unsteady flux of fluid through the slot Q is therefore greater (cf. (3.21) and (4.8)) as is the net rate of production/absorption of acoustic energy at the slot ((5.20) and (6.1)).

Similar trends are evident in figure 6 (*b*) (Case II) where $s/H = 0.5$ and $M = 0.05$, but for $\theta = \frac{6}{8}\pi$ or $\frac{5}{8}\pi$ insufficient energy is being produced at the slot to offset the acoustic energy Π_i, and the net incident flux Π_- is positive over the whole ks-range $0 < ks < 0.24$. The differences between the predictions for Δ, Cases I and II, are evident from figures 7 (*a*, *b*) (Case I) and figures 8 (*a*, *b*) (Case II), and are again most obvious when ks is very small and when the slot is producing acoustic energy. Those results also illustrate the influence on Δ of varying the ratio s/H and the Mach number M. Consider figures 7 (*a*) and 8 (*a*) ($M = 0.05$) for a particular s/H ratio. Acoustic energy is being produced at the slot in the region between the first and final ks-value at which Δ changes sign. Within that range two zeros of Π_- are again evident (i.e. $\Delta \sim -\infty$) and, in the region between, Π_- is negative. In figures 7 (*b*) and 8 (*b*) ($M = 0.1$) acoustic energy is absorbed at the slot over most of the ks-range 0–0.24; production occurs only in the small interval in which $\Delta < 0$.

7. Conclusions

Mean-flow/acoustic energy exchanges have been examined for the case of a thin rigid plate lying along the centreline of a duct and having a single slot, of width $2s$, by means of Howe's (1981*b*) linearized theory of shearing flow over a slot. Sound waves, of radian frequency ω, incident on the slot in the presence of equal low-subsonic grazing mean flows, of velocity U, on each side of the plate, generate vorticity which is shed from the leading edge of the slot and convected downstream with the mean flow. The acoustic energy absorbed in this process may be outweighed by that produced at the trailing edge of the slot by vorticity ejected into the flow, here modelled by displacement-thickness waves. Acoustic energy is absorbed at the slot provided the Strouhal number $\epsilon = \omega s/U$ is sufficiently small, but at higher frequencies there exists an infinite set of discrete frequency intervals in which a net amount of acoustic energy is generated, this energy being extracted from the mean flow.

The ratio of slot width to duct height influences the magnitude of energy exchanges but does not significantly affect their direction. When the influence of ejected vorticity at the trailing edge of the slot is neglected the linearized theory breaks down near that edge, where the displacement of the shear layer (vortex sheet) exhibits an inverse square-root singularity. This is reflected in the predictions of the acoustic-power production at the slot. Although qualitatively similar for certain ranges of ϵ, they diverge considerably from those which include the back reaction of ejected vorticity when $\epsilon \ll 1$ or when the mean-flow/acoustic interaction at the slot generates acoustic energy.

Predictions of the ratio of the total transmitted to incident flux for various s/H ratios, mean-flow Mach numbers and incident-wave phase differences, indicate that production of acoustic energy at the slot can result in a negative net incident power flux.

Appendix A. The Green functions $G_{\pm}(x, y_1)$

In the near field of the slot, $k|x| \ll 1$, $G_{\pm}(x, y_1)$ of (2.3) approximate line sources in an incompressible fluid at $x_1 = y_1$, $x_2 = 0\pm$ respectively, i.e. $G_{\pm}(x, y_1)$ satisfy

$$\left(\frac{\partial^2}{\partial x_1^2}+\frac{\partial^2}{\partial x_2^2}\right)G_{\pm}(x, y_1) = 0 \quad \cdot((kH)^2, kHM, M^2 \ll 1),$$

and the boundary conditions of (2.3). Use of the complex potential for such a source (Milne-Thompson 1968, §10.4) gives

$$G_{\pm}(x, y_1) = \frac{1}{\pi}\,\mathrm{Re}\left\{\ln\left[\sinh\left\{[x_1-y_1+\mathrm{j}x_2]\frac{\pi}{2H}\right\}\right]\right\}+c_{\pm}, \tag{A 1}$$

where Re denotes the real part with respect to the complex imaginary j. $c_{\pm}$ are complex constants chosen to satisfy the radiation condition that

$$G_{\pm} \sim A_{\pm}\,\mathrm{e}^{\mathrm{i}k|x_1|} \quad (k|x_1| \gtrsim O(1), \quad M \ll 1). \tag{A 2}$$

From (A 1)

$$G_{\pm} \sim c_{\pm}-\frac{\ln 2}{\pi}+\frac{|x_1|}{2H} \quad \left(|x_1| \gg \frac{2H}{\pi}\right). \tag{A 3}$$

In the region $1/k \gg |x_1| \gg 2H/\pi$, matching of (A 2), (A 3) yields

$$A_{\pm} = c_{\pm}-\frac{\ln 2}{\pi} = \frac{-\mathrm{i}}{2kH}. \tag{A 4}$$

The coefficients $c_{\pm}$ are purely imaginary and represent the leading-order effect of fluid compressibility, i.e. they account for radiation within the duct.

Appendix B. Evaluation of $\Theta_0(\chi_0)$, $\Theta_1(\chi_0, \xi)$, $f_m(\epsilon)$

Define

$$\left.\begin{aligned} \chi_0 &= -E+\chi_0^1 \\ \chi_0^1 &= (\beta+\alpha\xi)\,\mathrm{e}^{\mathrm{i}\epsilon\xi} = \left(\beta-\mathrm{i}\alpha\frac{\partial}{\partial\epsilon}\right)\mathrm{e}^{\mathrm{i}\epsilon\xi}. \end{aligned}\right\} \tag{B 1}$$

where, from (3.2) and (3.13),

From (3.6) and (3.10) and Gradshteyn & Ryzhik (1980, pp. 482, 973) we find

$$\left.\begin{aligned} &\Theta_0(-E) = -E, \quad \Theta_1(-E, \xi) = 0, \\ &\Theta_0(\chi_0^1) = \left(\beta-\mathrm{i}\alpha\frac{\partial}{\partial\epsilon}\right)J_0(\epsilon), \quad \Theta_1(\chi_0^1, \xi) = -\left(\beta-\mathrm{i}\alpha\frac{\partial}{\partial\epsilon}\right)\mathrm{i}\epsilon g(\epsilon, \xi). \end{aligned}\right\} \tag{B 2}$$

Here

$$\left.\begin{aligned} g(\epsilon, \xi) &= \xi J_0(\epsilon)+\mathrm{i}J_1(\epsilon)-2\sum_{k=1}^{\infty}\mathrm{i}^k J_k(\epsilon)\sin k\theta\sin\theta, \\ &|\xi| < 1, \quad \theta = \arccos(\xi). \end{aligned}\right\} \tag{B 3}$$

The definitions (3.10) and (B 3) give

$$\left.\begin{aligned} f_m(\epsilon) &= \mathrm{i}J_1(\epsilon)\,a_m + J_0(\epsilon)\,a_{m+1} - 2\sum_{k=1}^{\infty} \mathrm{i}^k J_k(\epsilon)\,h_k^m, \\ \text{where} \qquad h_k^m &= \frac{1}{\pi}\int_0^{\pi} (\cos\theta)^m \sin\theta \sin k\theta \,\mathrm{d}\theta. \end{aligned}\right\} \tag{B 4}$$

The h_k^m are evaluated with the aid of Gradshteyn & Ryzhik (1980, p. 374):

$$h_k^m = \begin{cases} 0\,(m < k-1, \quad \text{or } m+k \text{ even}), \\ [{}^m c_{\frac{1}{2}(m-k+1)} - {}^m c_{\frac{1}{2}(m-k-1)}]/2^{m+1} & (k+1 \leqslant m \quad \text{and} \quad m+k \text{ odd}), \\ {}^m c_{\frac{1}{2}(m-k+1)}/2^{m+1} & (k-1 \leqslant m < k+1 \quad \text{and} \quad m+k \text{ odd}) \end{cases} \tag{B 5}$$

${}^m c_j$ denote the binomial coefficients. In particular we find from (B 4), (B 5), (with $h_1^0 = \frac{1}{2}$, $h_2^1 = \frac{1}{4}$, $h_1^2 = h_3^2 = \frac{1}{8}$) that

$$f_0(\epsilon) = 0, \quad f_1(\epsilon) = J_1(\epsilon)/\epsilon, \quad f_2(\epsilon) = \mathrm{i}J_2(\epsilon)/\epsilon. \tag{B 6}$$

Appendix C. Evaluation of a_n, $b_n(\xi)$, d_n^m, $\Theta_0(\chi_1)$, $\Theta_1(\chi_1, \xi)$

From (3.10) and Gradshteyn & Ryzhik (1980, p. 374)

$$a_n = \begin{cases} 1 & (n = 0), \\ 0 & (n \text{ odd}), \\ {}^n c_{\frac{1}{2}n} & (n \text{ even}). \end{cases} \tag{C 1}$$

It follows from (3.10) and (C 1) that

$$b_n(\xi) = \begin{cases} -\xi & (n = 0), \\ \frac{1}{2} - \xi^2 & (n = 1), \\ \sum_{k=1}^{n} \{a_{n-k} - a_{n-k+2}\}\,\xi^{k-1} - \xi^{n+1} & (n > 1), \end{cases} \tag{C 2}$$

$$d_n^m = \begin{cases} -a_{m+1} & (n = 0), \\ -a_{m+2} + a_{m-2} & (n = 1), \\ \sum_{k=1}^{n} (a_{n-k} - a_{n-k+2})\,a_{n+k-1} - a_{m+n+1} & (n > 1). \end{cases} \tag{C 3}$$

Evaluation of $\Theta_0(\chi_1)$, $\Theta_1(\chi_1, \xi)$

From (2.20), (3.3) and (3.4) we find

$$\chi_1(\eta) = -\sum_{n=1}^{N} c_{2n} \sum_{r=0}^{2n} (-1)^r\, {}^{2n}c_r\, \eta^{2n-r} q_r.$$

Consequently

$$\frac{\partial \chi_1}{\partial \eta} = -\sum_{1}^{N} 2n\, c_{2n} \sum_{r=0}^{2n-1} (-1)^r\, {}^{2n-1}c_r\, \eta^{2n-r-1} q_r.$$

These expressions, (3.10) and (3.6) lead to the results

$$\Theta_0(\chi_1) = -\sum_{n=1}^{N} c_{2n} \sum_{r=0}^{2n} (-1)^r {}^{2n}c_r a_{2n-r} q_r,$$

$$\Theta_1(\chi_1, \xi) = -\sum_{n=1}^{N} 2n\, c_{2n} \sum_{r=0}^{2n-1} (-1)^r {}^{2n}c_r b_{2n-r-1}(\xi) q_r.$$

Rearrangement yields (3.12).

Appendix D. Evaluation of $\Theta_0(\Omega)$, $\Theta_1(\Omega, \xi)$, $\omega_m(\sigma)$

The functionals associated with Ω of (4.1) are calculated via the partition (4.7). Corresponding to the functional $\omega_m(\sigma)$ of (4.5) we define

$$\left.\begin{aligned} \omega_m(\sigma) &= \sum_{i=1}^{2} \omega_m^i(\sigma), \\ \omega_m^i(\sigma) &= \frac{1}{\pi}\int_{-1}^{+1} \frac{\xi^m \Theta_1(\Omega_i, \xi)}{(1-\xi^2)^{\frac{1}{2}}}\, \mathrm{d}\xi \quad (i = 1, 2). \end{aligned}\right\} \tag{D 1}$$

Evaluation of $\Theta_0(\Omega_1)$, $\Theta_1(\Omega_1, \xi)$, $\omega_m^1(\sigma)$

The functionals $\Theta_0(\Omega_1)$, $\Theta_1(\Omega_1, \xi)$ are determined in Howe (1981*b*) and are quoted here for ease of reference:

$$\Theta_0(\Omega_1) = -\frac{\pi}{2\sigma} H_0^{(1)}(\sigma) - \frac{\mathrm{i} \ln 2\mathrm{e}^{\mathrm{i}\sigma}}{i\sigma} \quad (\mathrm{Im}\,\sigma = 0_+), \tag{D 2}$$

$$\Theta_1(\Omega_1, \xi) = \mathrm{e}^{\mathrm{i}\sigma}\left\{\mathrm{i}I_1 + \xi I_0 - 2\sin\theta \sum_{n=1}^{\infty} \mathrm{i}^n \sin(n\theta)\, I_n\right\}, \tag{D 3}$$

where $|\xi| < 1$, $\theta = \arccos(\xi)$, and

$$I_n = \int_0^{\infty} \frac{J_n(k)\, \mathrm{e}^{-\mathrm{i}k}}{k-\sigma}\, \mathrm{d}k. \tag{D 4}$$

In particular

$$I_0 = \tfrac{1}{2}\pi\mathrm{i}\, H_0^{(1)}(\sigma)\, \mathrm{e}^{-\mathrm{i}\sigma}, \quad I_1 = \tfrac{1}{2}\pi\mathrm{i}\, H_1^{(1)}(\sigma)\, \mathrm{e}^{-\mathrm{i}\sigma} - \frac{1}{\sigma}. \tag{D 5}$$

$H_{0,1}^{(1)}$ are Hankel functions. The recurrence relationship

$$I_n = \frac{2(n-1)I_{n-1}}{\sigma} - I_{n-2} - \frac{2(-\mathrm{i})^{n-1}}{\sigma} \quad (n \geqslant 2), \tag{D 6}$$

follows from (D 4).

By analogy with $f_m(\epsilon)$ of Appendix B we find that

$$\omega_m^1(\sigma) = \mathrm{e}^{\mathrm{i}\sigma}\left\{\mathrm{i}I_1(\sigma)\, a_m + I_0\, a_{m+1} - 2\sum_{n=1}^{m+1} \mathrm{i}^n I_n(\sigma)\, h_n^m\right\}. \tag{D 7}$$

Evaluation of $\Theta_0(\Omega_2)$, $\Theta_1(\Omega_2, \xi)$, $\omega_m^2(\sigma)$

Ω_2 of (4.7) can be decomposed as

$$\Omega_2 = \Omega_3 + \Omega_4, \tag{D 8}$$

where, for $|\eta| < 1$,

$$\Omega_3(\sigma, \eta) = \int_\eta^\infty e^{i\sigma\tau} \ln\left\{\frac{\sinh[(\tau-\eta)\pi s/2H]}{[\tau-\eta]\pi s/2H}\right\} d\tau, \tag{D 9}$$

$$\Omega_4(\sigma, \eta) = -\int_\eta^1 e^{i\sigma\tau} \ln\left\{\frac{\sinh[(\tau-\eta)\pi s/2H]}{[\tau-\eta]\pi s/2H}\right\} d\tau$$

$$= -\int_\eta^1 e^{i\sigma\tau} P(\tau-\eta)\, d\tau, \tag{D 10}$$

(cf. (2.19)). Corresponding to (D 8) we set

$$\omega_m^2 = \omega_m^3 + \omega_m^4, \tag{D 11}$$

where ω_m^3, ω_m^4 are defined by (D 1).

By change of variable the integral Ω_3 may be expressed (Gradshteyn & Ryzhik 1980, p. 575) as

$$\left.\begin{aligned} \Omega_3(\sigma, \eta) &= -\frac{e^{i\sigma\eta}}{i\sigma}\mathscr{A}\left(\frac{\sigma H}{\pi s}\right) \quad (\mathrm{Im}\,\sigma = 0_+) \\ \text{where} \qquad \mathscr{A}(y) &= \ln y - \tfrac{1}{2}i\pi + \frac{1}{2iy} - \psi(-iy), \end{aligned}\right\} \tag{D 12}$$

and ψ is Euler's Psi function. By analogy with the corresponding functionals of χ_0^1 (Appendix B) we deduce that

$$\left.\begin{aligned} \Theta_0(\Omega_3) = -\frac{\mathscr{A}(\sigma H/\pi s) J_0(\sigma)}{i\sigma}, \quad \Theta_1(\Omega_3, \xi) &= \mathscr{A}\left(\frac{\sigma H}{\pi s}\right) g(\sigma, \xi), \\ \omega_m^3(\sigma) &= \mathscr{A}\left(\frac{\sigma H}{\pi s}\right) f_m(\sigma). \end{aligned}\right\} \tag{D 13}$$

The functionals $\Theta_0(\Omega_4)$, $\Theta_1(\Omega_4, \xi)$, ω_m^4 can be calculated from (D 10) and (2.20) for the polynomial P (truncated after N terms) in terms of the Bessel functions $J_n(\sigma)$. The calculation is not difficult but is too cumbersome for inclusion here. Details can be found in Quinn (1985).

REFERENCES

Abramowitz, M. & Stegun, I. A. 1964 *Handbook of Mathematical Functions*, 9th edn. Dover.

Bechert, D. W. 1979 Sound absorption caused by vorticity shedding, demonstrated with a jet flow. *AIAA Paper* 79–0575.

Blake, W. K. 1970 Turbulent boundary-layer wall-pressure fluctuations on smooth and rough walls. *J. Fluid Mech.* **44**, 637–660.

Blevins, R. D. 1984 Review of sound induced by vortex shedding from cylinders. *J. Sound Vib.* **92**, 455–470.

Bull, M. K. 1967 Wall pressure fluctuations associated with subsonic turbulent boundary layer flow. *J. Fluid Mech.* **28**, 719–754.

Carrier, G. F., Krook, M. & Pearson, C. E. 1966 *Functions of a Complex Variable*. McGraw-Hill.

Gradshteyn, I. S. & Ryzhik, I. M. 1980 *Tables of Integrals, Series and Products*. Academic Press.

Howe, M. S. 1980*a* The influence of vortex shedding on the diffraction of sound by a perforated screen. *J. Fluid Mech.* **97**, 641–653.

Howe, M. S. 1980*b* On the diffraction of sound by a screen with circular apertures in the presence of a low mach number grazing flow. *Proc. R. Soc. Lond.* A **370**, 523–555.

HOWE, M. S. 1981*a* The influence of mean shear on unsteady aperture flow, with application to acoustical diffraction and self-sustained gravity oscillations. *J. Fluid Mech.* **109**, 125–146.

HOWE, M. S. 1981*b* On the theory of unsteady shearing flow over a slot. *Phil. Trans. R. Soc. Lond.* A **303**, 151–180.

HOWE, M. S. 1981*c* The role of displacement thickness fluctuations in hydroacoustics, and the jet-drive mechanism of the flue organ pipe. *Proc. R. Soc. Lond.* A **374**, 543–568.

LIEPMANN, H. W. 1954 On the acoustic radiation from boundary layers and jets. Guggenheim Aeronautics Laboratory, California Institute of Technology, Pasadena.

LIGHTHILL, M. J. 1952 On sound generated aerodynamically: I. General theory. *Proc. R. Soc. Lond.* A **211**, 564–587.

MILNE–THOMPSON, L. M. 1968 *Theoretical Hydrodynamics*, 5th edn. Macmillan.

QUINN, M. C. 1985 Contributions to the theory of mean flow acoustic interactions in the presence of diffracting objects. Ph.D. thesis. University of Southampton, Faculty of Mathematical Studies.

VASUDEVAN, M. S., NELSON, P. A. & HOWE, M. S. 1985 An experimental study of the influence of mean flow on acoustic dissipation by vorticity production at edges. *IUTAM Symp. Aero- and Hydro-acoustics. Lyon. 3–5 July 1985.*

VÉR, I. L. 1982 Perforated baffles prevent flow-induced acoustic resonances in heat exchangers. In *Fortschritte der Akustik (FASE/DAGA '82)* Vol. 1, pp. 531–534. Göttingen.